



D4.2 – First report on bio-sourced materials & module components performance



Co-funded by
the European Union

Document control sheet

Project	RESiLEX – Resilient Enhancement for the Silicon Industry Leveraging the European matrix
Call identifier	HORIZON-CL4-2021-RESILIENCE-01-07
Grant Agreement Number	101058583
Coordinator	Iberian Sustainable Mining Cluster (ISMC)
Work package N°	4
Work package title	Sustainable, eco-design solar cells & modules
Work package leader	CSEM
Document title	D.4.2 - First report on bio-sourced materials & module components performance
Lead Beneficiary	CSEM
Dissemination level	Public
Authors	Timea Béjat, Lison Marthey, Adeline Lanterne, Laurie-Lou Senaud
Contributors	Agatha Lachowicz, Alexis Barrou
Reviewer(s)	CEA (Timea Bejat for CSEM parts), CSEM (Lison Marthey for CEA parts)
Issue date	April 2025

Version control table

Version	Date	Main changes
V1	10/04/2025	Frist Draft from CEA by Timea Béjat
V2	17/04/2025	Addition of CSEM parts by Lison Marthey
V3	24/04/2025	Compilation and addition of the last part on frame by Timea Bejat
V4	25/04/2025	Modification from CEA parts by Timea Bejat
V5	25/04/2025	Addition of introduction and conclusion by Timea Bejat
V6	26/04/2025	New contribution from Lison Marthey
V7	28/04/2025	Last review from Timea Bejat
V8	29/04/2025	Last review from Lison Marthey: VFINAL sent to ISMC
V9	06/10/2025	Addition of Version control table and reviewers' names

Index

1	Executive Summary	7
2	Introduction	8
3	Material selection and first development for low environmental impact BOM	9
3.1	Bio-based material screening of the market and first selection	9
3.2	Environmental impact associated with biobased materials for PV	13
3.3	Material Selection	14
3.4	Identified solutions for RESILEX integration	17
4	First study of the reliability and compatibility of new materials in PV module configuration	17
4.1	Material analysis: methods	17
4.2	Material processes and aging tests	20
4.3	Material analysis: results	21
4.4	CSEM: biobased materials implementation in modules	25
4.5	CEA: biobased materials implementation in modules	30
4.5.1	First testing campaign	30
4.5.2	Second testing campaign: integration of a bio-based polymer frontsheet	36
4.5.3	Frame	38
5	Conclusions	42
6	References	43

List of figures

Figure 1 Scheme of a conventional PV module stack.....	10
Figure 2 Strategy for the implementation of biobased materials in PV modules.....	12
Figure 3 Tensile strength and elongation at break of non-biodegradable biobased materials available on the market. Darker areas correspond to properties of conventional PV materials.	15
Figure 4 Workflow of material testing	18
Figure 5 Peeling configuration to test encapsulant’s adhesion to front and rear sheets	19
Figure 6 Total light transmittance of the used materials with reference solar glass data.....	22
Figure 7 a) Adhesion strength between the flax/PP backsheet and a commercial EVA or our internal PO. b) Pictured of a peeled sample showing that the delamination interface delamination is between the PP composite resin and the flax fibres.	23
Figure 8 Peeling test summary for CEA tests with both encapsulants, each stack was tested at glass and at BS interface	23
Figure 9 Workflow of peeling test campaign (at CEA).....	24
Figure 10 Schematic BoM of a) glass/backsheet modules with flax backsheet b) lightweight module with fluorinated frontsheet and flax backsheet.....	25
Figure 11 Performance of modules conventional flax backsheet in conventional and lightweight configurations	27
Figure 12 Efficiency losses of a) PERC flax and reference modules and b) IBC in thermal cycling.....	27
Figure 13 Efficiency losses of a) PERC flax and reference modules and b) IBC in damp heat.....	27
Figure 14 Lightweight module with a wood backsheet	28
Figure 15 CSEM module stack with non-fluorinated frontsheet, CSEM encapsulant that can be biobased and a biobased composite backsheet.....	28
Figure 16 a) Image and b) EL of modules with, from left to right PERC, SHJ and IBC cells.....	29
Figure 17: Power loss of modules after a) and b) DH for 2 times IEC	29
Figure 18 Isc losses after a) TC and b) DH	30
Figure 19 SHJ cell structure used for damp heat aging.....	31
Figure 20 Initial Pmax values of ten mono modules described in table 5.	32
Figure 21 Initial electroluminescence images of the ten studied mono modules.....	32
Figure 22 Variation in maximum module power output (Pmax) during DH aging – Cells with thin ITO	33
Figure 23 Variation in maximum module power output (Pmax) during DH aging – Cells with thick ITO.....	33

Figure 24 Variation in short circuit current (I_{sc}) during DH aging - Cells with 2 different ITO thicknesses 34

Figure 25 Variation in fill factor (FF) during DH aging - Cells with 2 different ITO thicknesses 34

Figure 26 EL images of the ten studied modules at 3000h of damp-heat aging 35

Figure 27 TPO2 module at intermediate measurement during DH aging 35

Figure 28 Optical microscope image of the delaminated interconnection on TPO2 module (TPO_ITO30_BS) 36

Figure 29 Lamination trials with polymer stack a) second trial with broken cells b) third trial with ameliorated lamination process with no cell break 37

Figure 30 EL images at initial and at 50 TC aging of the four modules 38

Figure 31 Both studied boundary conditions of the numerical study 39

Figure 32 Mesh optimisation in three stages with associated strength results 40

Figure 33 Simulation results of central deflection, max level of stress in cells and in glass 41

Figure 34 Wood knot where cracks form systematically 41

Figure 35: Finalized wooden frame 42

List of tables

Table 1 Boundary condition of aging test for material, mini module and full-size module level.....	20
Table 2 O2TR and WVTR of CSEM and commercial encapsulants and frontsheet.....	21
Table 3 Mechanical results of tested wood samples as frame material.....	25
Table 4 Visual inspection and EL images of the mini-modules with flax backsheet....	26
Table 5 Module bill-of-material (BOM)	31

1 Executive Summary

The photovoltaic industry is currently reaching an inflection point, positioning itself to become a major energy source. Optimizing its environmental impact is increasingly becoming a lever for industrial competitiveness, in order to sustain the sector's growth and address societal challenges. In this deliverable, we present the first results of a study focusing on the integration of bio-sourced materials into photovoltaic modules using silicon heterojunction cell (SHJ) technology.

After a brief introduction, we provide a comprehensive state-of-the-art analysis to map the availability and use of bio-sourced polymers for photovoltaic applications, with particular emphasis on the environmental impact analysis of these products. This analysis is followed by the material selection for the present study.

The next chapter covers several levels of analysis. We begin by presenting the material-level characterization, which allows us to define the process parameters for the subsequent integration into photovoltaic modules. Then, each involved research group presents the outcomes of these new materials integration into PV modules.

The document concludes with general conclusions and a list of bibliographic references.

2 Introduction

Cumulative photovoltaic deployment has reached the two terawatt scale in 2024 worldwide, and exponential growth is underway [1]. The photovoltaic industry is reaching the inflection point to become one of the major sources of energy, even dominant in certain regions. Optimizing the environmental impact of this technology is becoming a lever for industrial competitiveness and for maintaining the sector's growth, as well as responding to societal challenges. National and European legislations, as well as industry alliances, strongly support the implementation of an eco - design approach. Pioneering European manufacturers (REc, Bisol, Qcells, Voltec) are beginning to offer low - carbon photovoltaic panels. Reducing environmental impact is also an important differentiating factor versus existing products. The aim of this task within the work package 4 is to manufacture PV cells and modules with 50 % reduced carbon footprint and a reduce consumption of critical material such as Ag and In in the manufacturing of heterojunction (SHJ) solar cells without compromising efficiency. With this objective in mind, the establishment of an eco - design approach enables us to work jointly on cell technologies, interconnection and BOM (bill - of - material) selection to achieve this performance.

In the deliverable D4.1 on the *Interim roadmap for Eco-design of silicon solar cell module* we have highlighted that the aluminium (Al) frame and the glass are the highest contributors to the CO₂ footprint for module manufacturing [2], making their substitution evaluation the most relevant. We also highlighted that conventional backsheets and some polymer frontsheets present on the market contain fluoropolymers which necessitate specific equipment for the module end of life, resulting in higher costs of the recycling process compared to non-fluorinated materials.

This report aims to evaluate the introduction of *biobased* materials and other lower impact materials in photovoltaic (PV) modules as substitutes for conventional materials.

3 Material selection and first development for low environmental impact BOM

3.1 Bio-based material screening of the market and first selection

Biobased materials, produced from renewable feedstocks, potentially offer a lower environmental footprint compared to energy-intensive or fossil-based materials, thereby reducing reliance on fossil resources. Our approach involves assessing the substitution of conventional PV module materials with biobased alternatives in terms of *performance, reliability, and environmental impact*.

Definitions

Biobased materials are completely or partially derived from biomass. These materials have a *bio-content* percentage that indicates the share of carbon atoms originating from biomass. Biobased materials should not be confused with biodegradable materials which can be decomposed into smaller molecules by living organisms in various environments.

There are different types of biobased materials. First, there are *natural materials* such as wood, natural fibres or rubber that are not processed. Then, there are bio-based polymers. Drop-in polymers are chemically equivalent to their fossil-based counterparts but are derived from biomass; for example, bio-poly-ethylene (PE) or bio- polyethylene terephthalate (PET) have the same molecular chains as conventional fossil-based PE or PET. In contrast, there are bio-based polymer that do not have fossil-based equivalents, such as polylactic acid (PLA) or polyethylene furanoate (PEF).

Another type of biobased materials that can be use are the *bio-composites*, they either include a bioplastic matrix or biobased fibres/fillers or a combination of both.

Conventional PV module structure

Prior to substituting conventional PV materials, it is essential to thoroughly understand the functions and properties of each constituent within a PV module.

A PV module comprise a stack of active and protective materials. The core of the device consists of the interconnected silicon cells, or strings, that convert light into electricity. As illustrated in Figure 1, these cells are encapsulated with polymeric *encapsulant*,

glass at the front, and either a *backsheet* or *glass* at the rear. This packaging is crucial for protecting against weathering and maintaining the structural integrity of the cells. The *front cover*, typically made of glass, has high transmittance, acts as a barrier to moisture and oxygen ingress, and in addition provides mechanical stability while protecting the cells from impact.

The *encapsulant* is a transparent polymer sheet, usually polyolefin elastomers (POE) or ethylene-vinyl acetate (EVA) [3], that bonds the different elements of the module, accommodate mechanical stress and electrically insulate the solar cell.

The *rear cover* delays moisture ingress and external gases while providing electrical insulation. It can be made of glass or a multi-layered polymeric foil known as backsheet. The core layer of the backsheet is generally PET and contains fluoropolymer layers. Other backsheets may use alternative materials such as polyolefin (PO) or polyamide (PA) to avoid the use of fluorine [4].

Finally, a *frame* is added, it offers a structural support and serves as fixation system, typically made of aluminium.

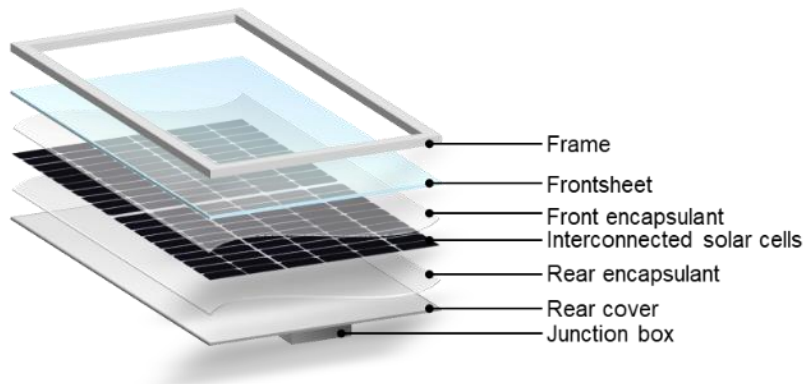


Figure 1 Scheme of a conventional PV module stack

For specific applications requiring low-weight PV modules, such as vehicle-integrated PV or roofs with limited load-bearing capacity, lightweight PV modules can be produced. This can be achieved by using either thinner glass or polymer as the frontsheet, combined with a rigid (often composite) layer for the rear side.

Literature review

A literature review on the substitution of conventional *PV modules components* with biobased materials has been conducted. It is important to note that components of organic (non-Si) PV cells can be substituted with bio-based materials [5] however this is beyond the scope of this work.

The backsheet is the most extensively assessed module element for biobased substitution, with researchers evaluating the use of PLA as a backsheet material. PLA is a biodegradable material [5], [6] with low thermal degradation temperature [8]. During testing for PV application, the material decomposed [9], cracked or peeled [10] under damp heat (DH) conditions (85 °C, 85 % RH) which makes it unsuitable for conventional PV applications.

PA11 has also been studied [8], [10], [11], [12]. Derived from castor bean oil feedstock, PA11 is non-biodegradable. The company biosolar developed a final product incorporating mica and talc fillers which reduce the water vapour transmission rate (WVTR). Measurements of bond strength and thermal conductivity, along with DH tests, have shown promising results [8], [10]. However, it is important to note that conventional backsheets made with PA are not ideal for field deployment due to their tendency to embrittlement in outdoor conditions [14].

Additionally, a drop-in bio-PET was tested by a team of Fraunhofer CSP [13], the modules exhibited encouraging reliability results following IEC61215 [15] & IEC61370 [16] standards. Nevertheless, under damp heat conditions the modules experienced degradation. This degradation may not be solely attributed to the bio-PET backsheet but could be due to the biodegradable EVA incorporated in the module.

Furthermore, the use of natural fibre composites has also been evaluated. In particular, a composite made of PLA with vetiver fibres [8], polyvinylidene fluoride (PVDF) with reinforced short sugar palm fibres [16], [17] and high-density polyethylene HDPE mixed with various natural fibres such as staghorn sumac, pomegranate and black pepper [19]. The electrical performance of the modules were reasonable [16], [17] with some results showing enhanced open circuit voltage due to the improved temperature distribution. However, the reliability of these modules were not tested [19].

Similarly, biobased encapsulants have also been evaluated, though less commonly studied. Commercially available bio-PE or a biobased thermoplastic polyether block amide elastomer (TPA) are possible candidates [12] but these materials do not fulfil the requirements in terms of mechanical performance [20] and long term stability. The materials mentioned have however the potential to achieve long term stability through modification and stabilization. Additionally, natural dyes extracted from plants can be used as additives. Wheat husk, turmeric rhizomes and moringa leaves contain luminescent downshifting dyes and have the potential to enhance the performance of the PV module [21].

Wooden frames have been proposed as a viable alternative to conventional aluminium frames [21], [22]. Following the Si-cell, the Al frame has the highest carbon contribution

to the overall module. Substituting aluminium with wood reduces the environmental impact and appears to be a promising approach. However, further research is needed to fully understand the durability of such assemblies [21], [22].

Materials selection strategy

Given that research on biobased materials for PV is still in its preliminary stages and some studies lack sufficient qualification for PV applications, a practical framework for material selection strategy is proposed in this work. Figure 2 presents this methodology on a graphical way.

- 1) Define the targeted element to be substituted with a biobased material, along with the goals and constraints of the substitution. Constraints may include properties, cost, environmental impact, commercial availability, etc.
- 2) Perform an inventory of existing biobased materials, sourced from an up-to-date database or through a dedicated supplier search.
- 3) Screen the material inventory according to the defined constraints.
- 4) Conduct various characterization methods to assess mechanical, optical, and thermomechanical properties after preliminary screening. If an extended lifetime is targeted, biodegradable materials are excluded a priori.
- 5) Perform a Life Cycle Assessment (LCA) to evaluate the environmental impact of a product across 16 different impact categories (e.g., carbon emissions, water resource consumption, ecotoxicity). For a PV module, carbon emissions are measured based on the amount of solar electricity generated (kWh) or the module / system's nominal capacity (kWp). Conducting an LCA now can help eliminate fewer promising materials and save effort.
- 6) Characterize and qualify new materials to meet PV requirements using IEC standards. Key evaluation criteria include safety, optical properties, durability, accelerated weatherability, and adhesion between components.
- 7) Once qualified, implement the materials into the module and test them according to qualification standards.

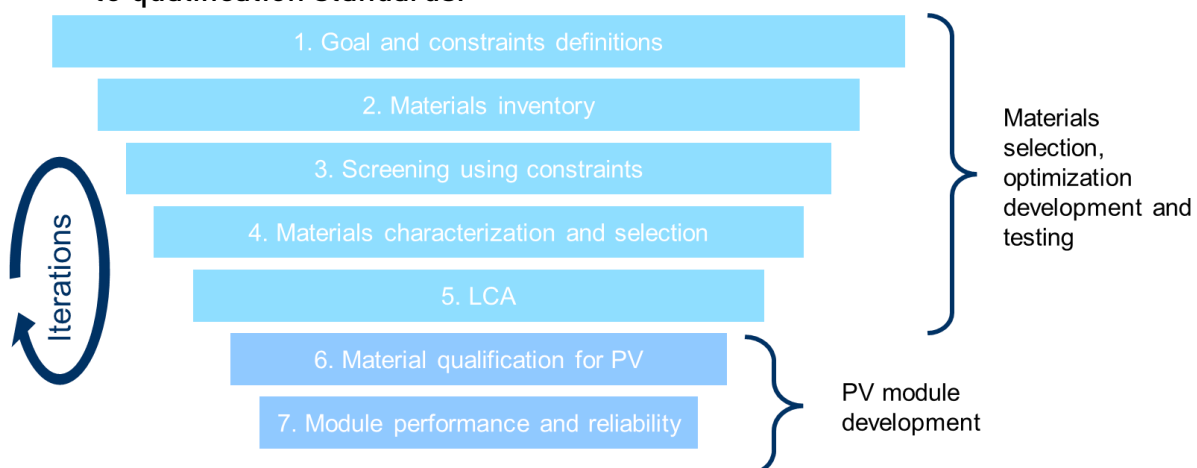


Figure 2 Strategy for the implementation of biobased materials in PV modules

3.2 Environmental impact associated with biobased materials for PV

The literature lacks extensive critical discussion on the environmental benefits or changes associated with substituting conventional materials with biobased materials. This section addresses this gap.

Biobased polymers

Produced from renewable feedstocks, bio-based polymers potentially exhibit a lower environmental footprint compared to fossil-based plastics due to biogenic carbon removal and reduce reliance on fossil resources. However, this environmental benefit can come with trade-offs in terms of other life cycle assessment impact categories and can increase the risk of burdens shifting. Additionally, first generation feedstocks such as corn and sugarcane, are controversial due to potential competition with food resources.

In a review, Walker & Rothman discuss the challenges associated with introducing bioplastics in the economy [24]. The authors note that most studies focus on the global warming potential and energy depletion while other impact categories receive less attention. Furthermore, the LCA studies on the topic do not have cohesive conclusions, reflecting the discrepancy in study methodologies and highlights the limitation of LCA when comparisons are not feasible.

Additionally, considering the potential environmental benefits, the use of biobased polymers raises the question of the land and water required to produce such materials. These values are currently being evaluated.

When discussing the substitution fossil-based for bio-based polymers in PV applications, it is essential to acknowledge the uncertainties regarding their environmental impact improvements.

Wood

Historically photovoltaic modules have aluminium frame. Aluminium has the second highest impact on the carbon footprint of a PV module. Its substitution by a timber frame decreases the module's carbon footprint. Aluminium frame substitution with wood appears to be a suitable solution in term of mechanical properties but also for greenhouse gases emissions [21], [22]. This replacement requires a frame section development as wood has lower mechanical strength than aluminium. As frame material, the wood's most important characteristics are the mechanical strength, the durability, fire resistance needs to last as long as the rest of the module and

maintaining the overall structure. O&M costs should be considered linked to wood degradation prevention.

Bio-composites

Composites in general can be used as backsheet for lightweight PV products. Bio-based composites are a combination of bio-based polymers and/or natural fibres / fillers, providing an alternative to conventional composites. In terms of mechanical performance bio-composites can be comparable to their fossil-based counterpart exhibiting high stiffness, moderate strength and low density. Natural fibres are competitive alternatives for synthetic fibres. However, most natural fibres underperform in long-term durability [25] and exhibit unclear structural stability [26]. Additionally, the resin used in bio-based composites significantly influences their environmental impact [26]. While plant fibres can have a lower impact compared to synthetic fibres, current technologies require more resin for plant based fibres, potentially offsetting the environmental benefit of using natural fibres [26].

Module level impact

As outlined in the material selection strategy, the environmental impact of a PV system can be measured in two ways: kWp, which pertains to module manufacturing, and kWh, which reflects the environmental impact of the electricity generated by PV systems.

The environmental impact per kWh depends on the module's performance and lifetime, both of which are crucial factors. Therefore, any new material must not only be environmentally superior at the material level but also maintain the initial performance and reliability of the PV module. This trade-off must be carefully considered.

To conclude this section, as discussed in the previous sections, the environmental performance of bio-based materials at the material level is not always guaranteed. Additionally, substitution does not necessarily ensure a lower impact of electricity production, which depends on the performance and lifespan of the module. Therefore, all these factors must be considered when making material choices.

3.3 Material Selection

Materials screening

For substitution of conventional PV polymer with biobased polymers, an initial screening was conducted following the materials selection methodology. The goal was to substitute conventional PV materials (i.e., backsheet, encapsulant, and frontsheet) with bio-based polymers while preserving module performance and reliability. The constraints were defined as follows: the materials must be commercially available and

processable as foil. Biodegradable materials were excluded due to their uncertain long-term outdoor stability.

To compile the material inventory, an online search was conducted to gather technical datasheets of bio-based materials. The preliminary screening, performed in collaboration with PCCL¹, identified 143 non-biodegradable, bio-based, and commercially available polymers, including different grades of the same material. Their bio-content ranged from 10 % to 100 %.

These materials were then screened based on constraints, comparing their elongation at break and tensile strength from the technical datasheets to those of the corresponding target materials for substitution. The results are summarized in Figure 3. Each marker represents bio-based materials, while the coloured areas indicate the required properties of conventional materials [4]).

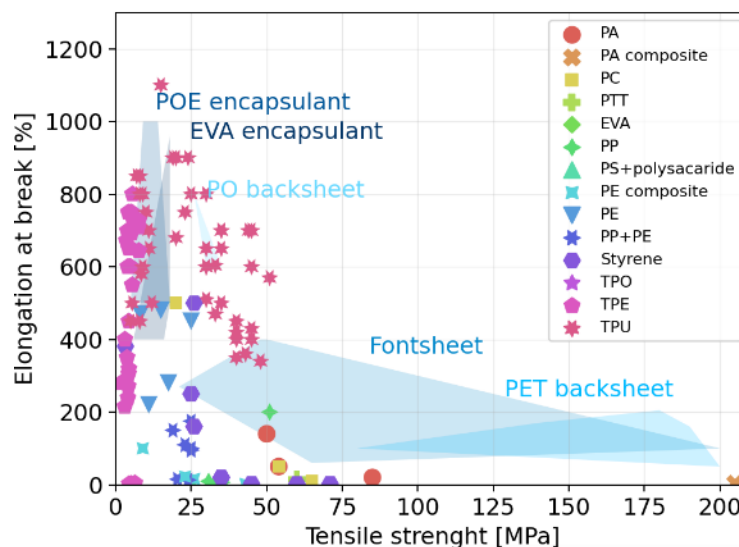


Figure 3 Tensile strength and elongation at break of non-biodegradable biobased materials available on the market. Darker areas correspond to properties of conventional PV materials.

The screening results indicate that a few bio-based polymers may possess adequate mechanical properties. However, not all these polymers can be processed into polymer sheets, which is essential for PV applications. Additionally, for encapsulant and frontsheet applications, the materials must be transparent. No bio-based EVA or POE drop-ins were found. Thermoplastic polyurethane (TPU) appears to be suitable for substituting PO backsheets or encapsulants.

While some of these materials showed potential, for the encapsulant we ultimately decided to use a polymer that, although not currently biobased, possesses superior properties and can be produced from biobased sources in the future. This decision was

¹ PCCL : Polymer Competence Center Leoben, Austria

made to ensure optimal performance and durability of the final product, while keeping the door open for future sustainability improvements.

Encapsulant Selection

For the encapsulant, we selected a silane-grafted resin that has the potential to be biobased. This resin is ideal for PV encapsulation due to its transparency and its ability to cross-link with moisture, enhancing reliability. This material properties can be fine-tuned at CSEM thanks to polymer formulation know - how. The encapsulant can be formulated to be adapted for different bill of materials, including composite backsheets.

Backsheet selection

Polyethylene furanoate (PEF), a bio-based material, was initially considered for use as a backsheet or frontsheet. This polymer has properties like PET (a conventional backsheet material) and even offers improved barrier properties. Unfortunately, the sole supplier could not provide samples to perform developments in this project.

For lightweight applications, rigid composite backsheets containing natural fibres were selected. The first promising bio-sourced composite under investigation is a film made from woven natural flax fibres and a polypropylene (PP) thermoplastic resin. A key advantage of this composite is that the PP thermoplastic resin can be recycled, unlike the epoxy resins commonly used in composite materials. According to supplier information, the flax fibres can be embedded in either fossil-based PP or PLA. However, even if PLA is a biodegradable material, studies have shown that PLA materials/modules fail in damp heat (DH) tests for PV applications, that is why the PP was chosen for the developments of this project.

In parallel we have also selected and investigated thin wood planks as backsheet in lightweight configuration.

Frontsheet selection

A polymer, flexible non fluorinated frontsheet was developed at CSEM and extruded. The strength of this front sheet lies in its non-fluorinated composition, even though it is not bio-based. Due to its flexibility, this frontsheet requires a rigid backsheet to provide mechanical stability to the module. The frontsheet was tested in combination with the flax backsheet previously described.

Frame

Material selection is based on the quality, hardness, weather resistance of various wooden types. Five wood species were targeted: the acacia, the oak, the chestnut, the spruce and a tropical species the opepe (bilinga). The chosen species are all,

theoretically, without maintenance and no need of treatments during service life. Wood may be chosen according to national requirements covering durability issues corresponding to outdoor use, without ground contact and with exposure to weathering.

3.4 Identified solutions for RESILEX integration

Following material level testing we carried out module level testing (accelerated aging). The bill-of-material (BOM) including as many bio-sourced material as possible was:

- Non fluorinated frontsheet (CSEM) bio-based frontsheet (CEA) or low CO₂ glass (thinner and EU sourcing)
- Encapsulant: bio-sourced of the project (CSEM)
- Backsheet: bio-sourced/recycled
- Frame: bio-based (wood).

Solar cells included in project's tested modules were supplied by other tasks of work package 4 with reduced Indium and silver content.

4 First study of the reliability and compatibility of new materials in PV module configuration

4.1 Material analysis: methods

Once first version of the bio-based materials had been acquired, material level test may start following the presented steps in Figure 4. Each test might give information on material performance compared to reference (already known) materials and could eliminate or confirm candidate bio-based materials for further PV module integration. In the following, each type of analysis is presented.

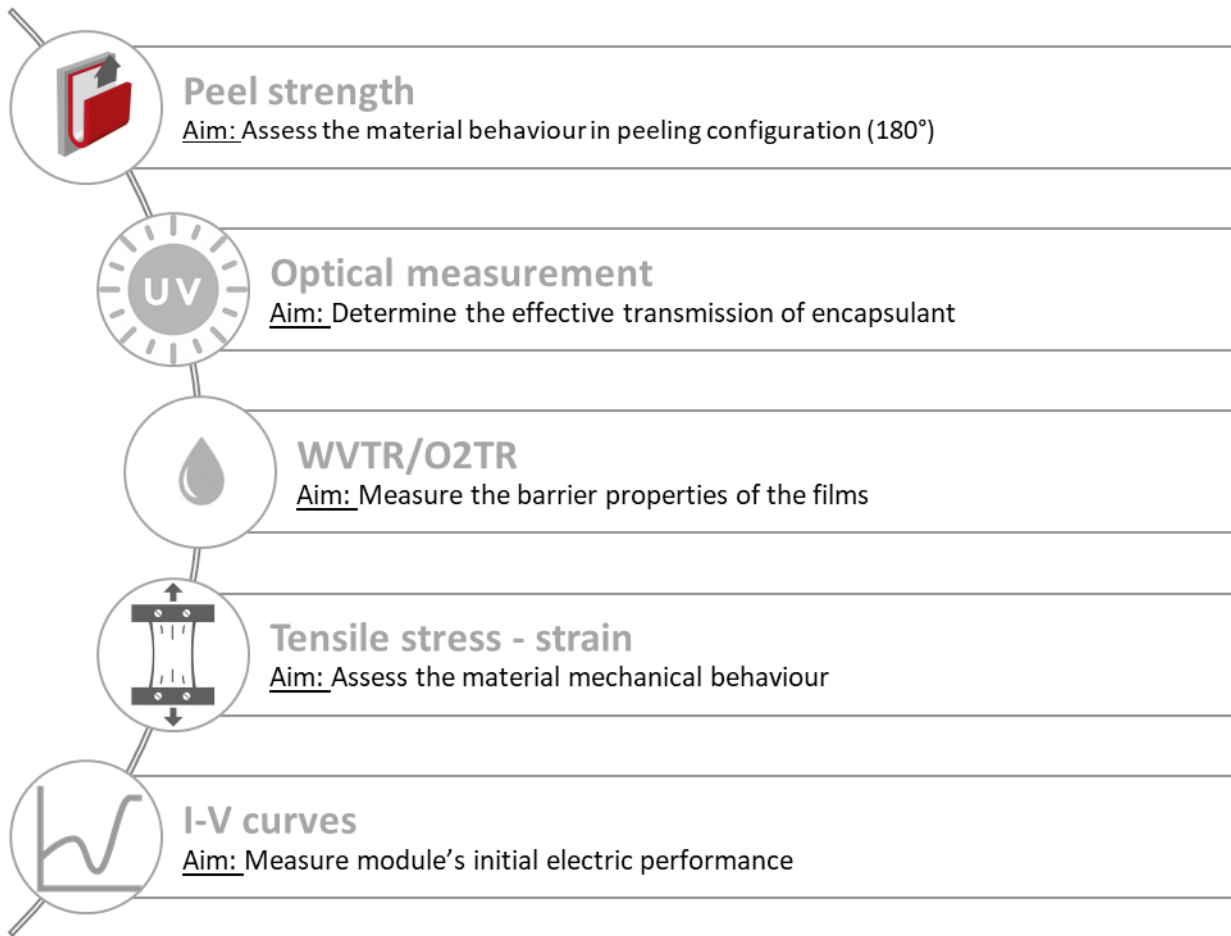


Figure 4 Workflow of material testing

Peeling

Bonding between module materials had been tested by peeling 180 °with an Instron 3365 device on 20 cm x 20 cm samples at CEA and with a Zwick tensile test machine in 90°, on 20cm x 2.5cm samples at CSEM. Special samples had been laminated expressly for these tests. Figure 5 presents samples' configuration according to the tested interface in 180 ° configuration.

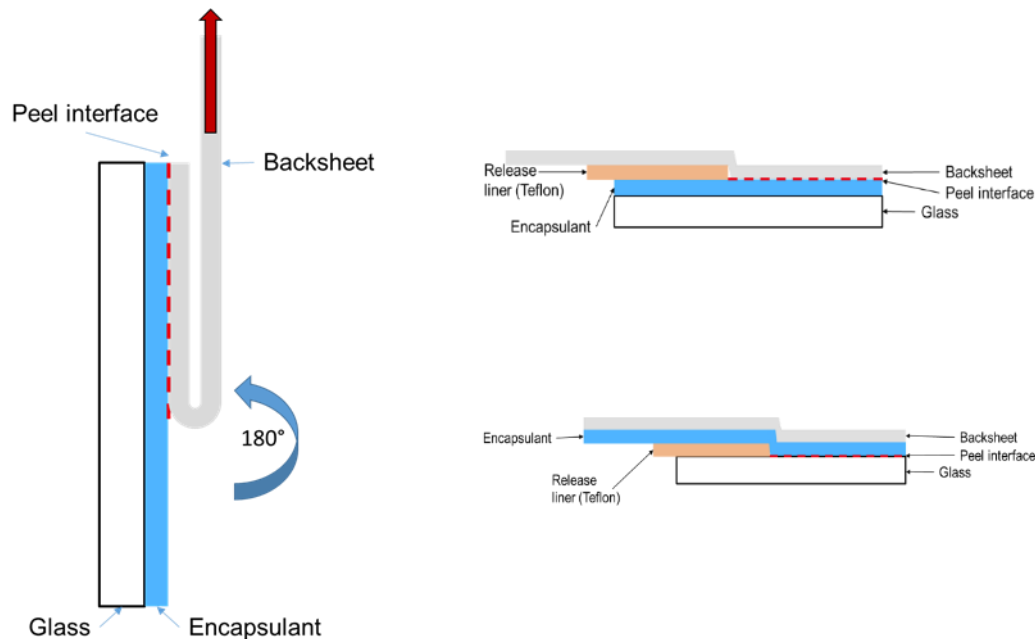


Figure 5 Peeling configuration to test encapsulant's adhesion to front and rear sheets

Transparency measurement

The total transmittance was measured at CEA using a Perkin Elmer lambda 950 UV/VIS/NIR spectrometer equipped with a Deuterium lamp. Spectra were acquired in the 300 – 1200 nm wavelength range on samples using 10 nm increment. Measurements and used device are in accordance with the IEC 62788-1-4 standard.

Barrier properties

Oxygen transmission rate (O₂TR) in cm³/m².day and water vapour transmission rate (WVTR) in g/m².day measurements were performed and compared to those of commercial conventional frontsheet and encapsulants. They are two important parameters for PV module's reliability. O₂TR measures how much oxygen permeates through a material, while WVTR measures the permeation of water vapor. In both measurements, the material sample is placed between two chambers: one with controlled atmosphere and the other with a flow of nitrogen gas. The nitrogen chamber has a detector that measures the amount of water vapor or oxygen that has passed through the sample over time.

Tensile stress – strain

Assessment of material's mechanical performance on an Instron 3365 device to determine young modulus for numerical simulation. We applied a force on four point bending test and recorded the displacement to determine material's stress.

PV module initial performance characterisation

The I-V measurements are conducted at room temperature (21 – 24 °C) on a A+A+A+ flash tester with a flash duration of 250 ms. A temperature correction is done to obtain the measurements at 25 °C. The I-V results are obtained for standard test conditions (1000 W / m², AM1.5G and 25 °C). Electroluminescence imaging (EL) is captured with a GreatEyes CCD Silicium camera at 1 sun equivalent current injection. Samples are measured at their initial stage and at regular intervals during ageing test for both types of measurement.

4.2 Material processes and aging tests

Flax backsheet process:

Before sample or module implementation, the composite must be processed. Indeed, the material is received as a roll of woven flax fibres impregnated with PP. The composite film is heated to a temperature above the melting point of the PP resin and then subjected to a pressure to ensure proper impregnation of the flax fibres. To reach an appropriate rigidity, the backsheet is composed of several layers of the composite film.

Frontsheet and encapsulant process

At CSEM we have our own extruder, we can formulate polymer sheets choosing the adapted resin and additives. PV encapsulant extrusion involves feeding the base resin and additives into an extruder, where it is heated and melted. The molten material is then forced through a die to form a continuous sheet. This sheet is subsequently cooled and solidifies. The encapsulant film is then ready to be laminated onto the PV module. In this work we have developed a polymeric encapsulant that can be biobased and a non-fluorinated polymeric frontsheet thanks to this process.

Accelerated aging test

We used the international standard's [15] requirements to fix ageing boundary conditions. It was adopted for all level of testing presented in this paper, from material level up to full size modules. The only difference remains in the duration of the exposure that is adapted to the special needs of each studied parameter. We summarized the measurement conditions in Table 1.

Table 1 Boundary condition of aging test for material, mini module and full-size module level.

Aging test	Irradiation [kWh/m ²]	Temperature [°C]	Relative Humidity [%]
UV	60	60	Not controlled
Damp Heat (DH)	-	85	85
Thermal cycling (TC)	-	-40 C° - 85 C°	Not controlled
Humidity-Freeze	-	-40 C° - 85 C°	85

4.3 Material analysis: results

Encapsulant and frontsheet

As discussed in previous section, the barrier properties of PV materials are crucial. Two important parameters are the water vapor transmission rate (WVTR) and the oxygen transmission rate (O2TR).

As shown in Table 2, the barrier properties of the CSEM fluorine free frontsheet are superior to those of fluorinated commercial frontsheet, particularly in terms of WVTR. Additionally, the CSEM encapsulant performs similarly to conventional POE.

Table 2 O2TR and WVTR of CSEM and commercial encapsulants and frontsheet

Type	O2TR [cm ³ /m ² .day] 40°C/90% RH/ 21% O ₂	WVTR [g/m ² .day] 50°C/ 90% RH
CSEM frontsheet	87	4.18
Fluorinated frontsheet	159	13.52
CSEM encapsulant	800	4.16
POE	730	3.45
EVA	410	13.52
EPE	434	3.63

The transmittance of the frontsheet and encapsulant is crucial for module performance. The developed frontsheet blocks UV radiations, and there are two versions of the encapsulant: one that cuts UV (CSEM TPOUV) and one that allows UV through (CSEM TPO). In the RESILEX project, the targeted cell is the SHJ, which is known to be sensitive to UV exposure. Therefore, UV-cut materials are preferred. Figure 6 presents total light transmittance results of polymer frontsheet studied at CEA, CSEM TPOUV encapsulant and a reference solar glass. The frontsheet and the encapsulant block UV light while reference glass not. Encapsulant has a better optical performance than the polymer frontsheet.

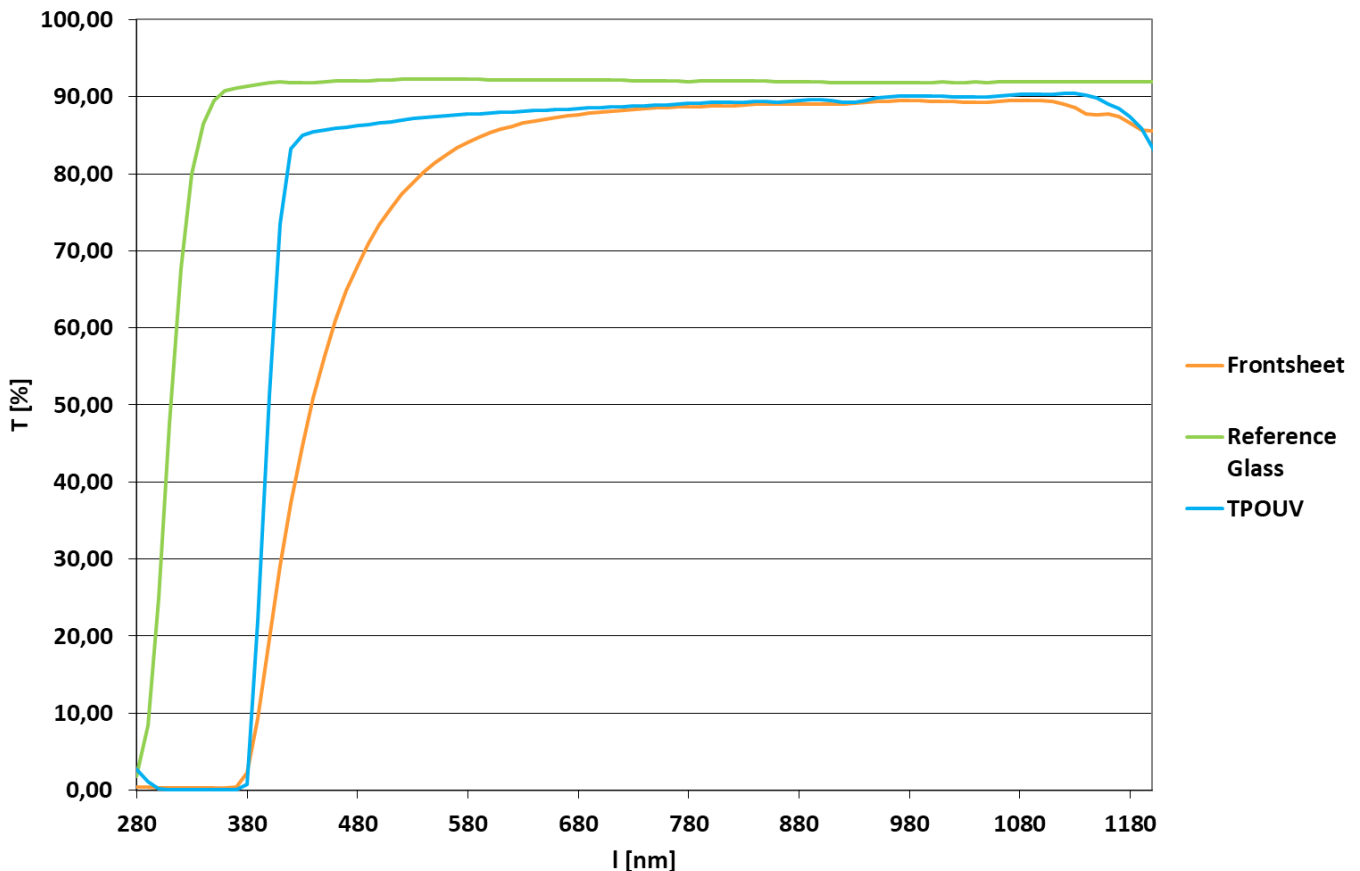


Figure 6 Total light transmittance of the used materials with reference solar glass data

Backsheet

As an initial investigation, the flax backsheet was subjected to damp heat (85 °C, 85 % RH) for 1000 hours. It successfully demonstrated no interlayer delamination and remained intact. However, the natural fibres showed moisture absorption. Given that CSEM encapsulant has a low WVTR which could delay moisture ingress, the decision was made to proceed with the PP / flax backsheet.

As a first step, the compatibility of the encapsulant with the flax backsheet was tested. Ensuring adhesion between the layers is crucial for the module's reliability. The adhesion between the flax backsheet and different encapsulants was evaluated using the 90 ° peel test method. Both commercial EVA encapsulant and CSEM encapsulant were assessed.

The results, shown in Figure 7, indicate that both materials have similar adhesion strengths between 20 and 30 N / cm, which is lower than the intended 60 N / cm. For both encapsulant types, the delamination interface appears to be within the composite itself, at the PP resin / flax fibres interface. After 1000 hours in damp heat (DH), this value drops to 15 N / cm.

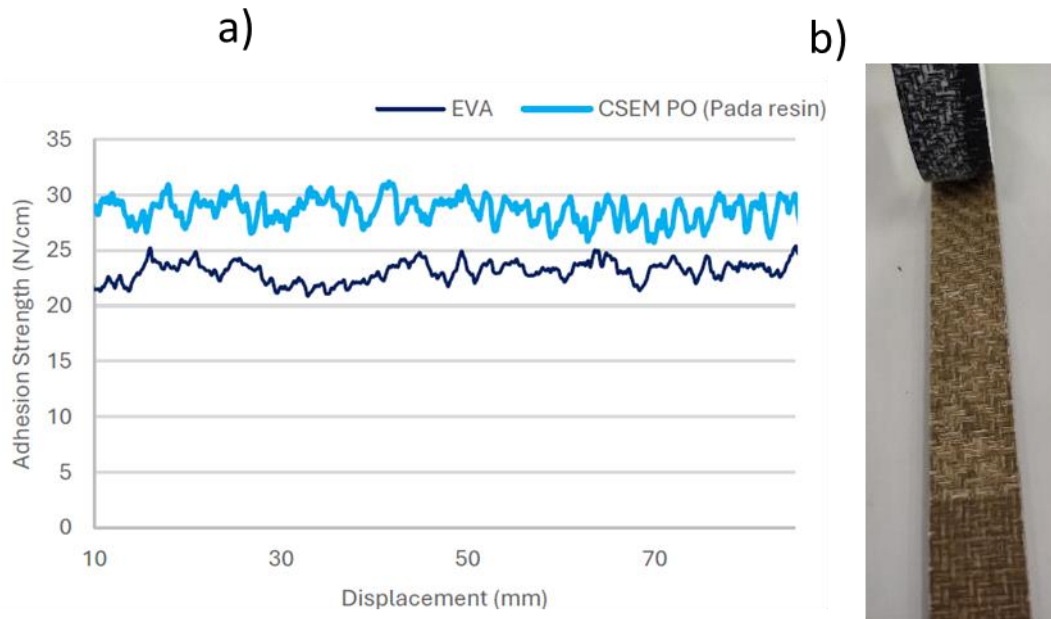


Figure 7 a) Adhesion strength between the flax/PP backsheet and a commercial EVA or our internal PO. b) Pictured of a peeled sample showing that the delamination interface delamination is between the PP composite resin and the flax fibres.

Encapsulant and backsheet bonding

In a first time, first version of project’s encapsulants were tested in combination of two commercially available backsheets: one PP, and one European aluminium containing PET core backsheet reference. Figure 8 presents the possible combinations between the tested interfaces and the bill-of-material (BOM).

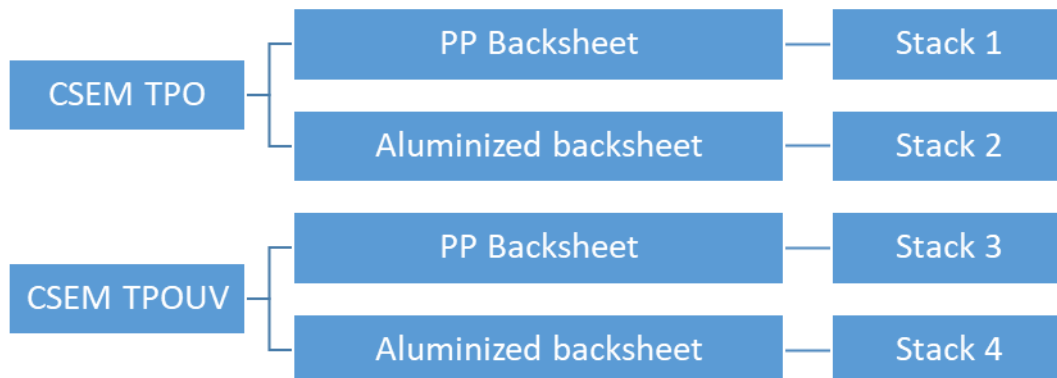


Figure 8 Peeling test summary for CEA tests with both encapsulants, each stack was tested at glass and at BS interface

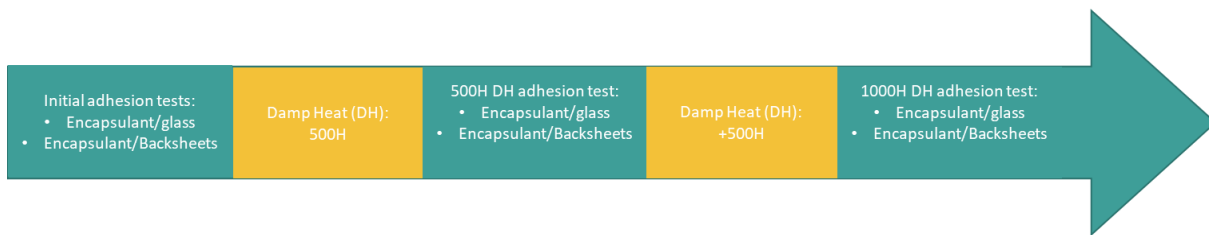


Figure 9 Workflow of peeling test campaign (at CEA)

Figure 9 presents the workflow of the peeling test campaign at CEA. As a first trial, a polypropylene (PP) backsheet was tested with project encapsulant as an eco-friendly solution (no fluorine no aluminium content). This PP backsheet could be further on substituted with a bio-based material with close mechanical properties. As presented above, a European aluminium containing PET core backsheet was tested as reference. As showed in Figure 8, we carried out several peeling tests. Initial values were recorded right after sample lamination. Then measured samples had been sent to damp heat (DH) aging for 500 h, peeling test repeated, and samples continued aging for next 500 h in DH. Final measurements give information about the adhesion between the layers after 1000 h of DH aging of the samples (Figure 9). These values indicate potential failure if they remain under target value. We used these tests to assess lamination recipe efficiency too. The following list presents a global appreciation of this peeling test campaign:

Stack1: Glass / CSEM TPO / PP BS

- T0: 67 N / cm / 500h: 20 N / cm / 1000h: 21 N / cm

Stack2: Glass / CSEM TPO / PET Al BS

- T0: 165 N / cm / 500h: 95 N / cm / 1000h: 85 N / cm.

Stack3: Glass / CSEM TPOUV / PP BS

- T0: 75 N / cm / 500h: 20 N / cm / 1 000h: 18 N / cm

Stack4: Glass / CSEM TPOUV / PET Al BS

- T0: 140 N / cm / 500h: 90 N / cm / 1000h: 90 N / cm

As adhesion forces are largely higher between project encapsulants and PET core aluminium containing backsheet we kept Stack2 and Stack4 for further tests and module integration: adhesion forces, even after 1000 h of DH aging, of tested samples are over internal limit forces (corresponding to manufacturer's suggestion too).

Frame

Wood species from inventory must undergo material level testing to validate their frame integration. Mechanical properties and frame section dimensioning precede the validation of the final solution: we used four points bending to obtain young modulus

and tensile strength on frame elements before and after accelerated ageing tests (thermal cycling and humidity freeze tests). Table 3 summaries the obtained results.

Table 3 Mechanical results of tested wood samples as frame material

Frame material	Flexural strength (MPa)			Young modulus (GPa)		
	Initial stage	After TC	After HF	Initial stage	After TC	After HF
Aluminium	62	-	-	46.3	-	-
Acacia	120±18	130±3	120±29	22±0,8	21±1,2	21±1,2
Chestnut	120±6	110±22	100±14	21±1	19±0,8	27±1,4
Oak	110±5	140±0	110±13	17±1,8	22±0	23±3,8
Opope (Bilinga)	100±32	80±25	80±35	20±3	16±4,3	19±4,9
Spruce	70±12	80±34	60±11	19±0,6	19±4,5	18±4,6

From this step of testing, we kept only one wood species, the acacia, which had the best performance in flexural strength measurements after humidity / freeze aging. This wood species is a local variety and abundantly available in Europe.

4.4 CSEM: biobased materials implementation in modules

Preliminary tests

To evaluate the performance and reliability of PV modules integrating the developed flax backsheets and the CSEM encapsulant, mini modules were processed using two half cells. Their Bill of Materials (BoM) is shown in Figure 10. One module is conventional, featuring a flax backsheet, front glass, and CSEM encapsulant. The other module is lightweight, with a flax backsheet on the rear side and a fluorinated commercial frontsheet.

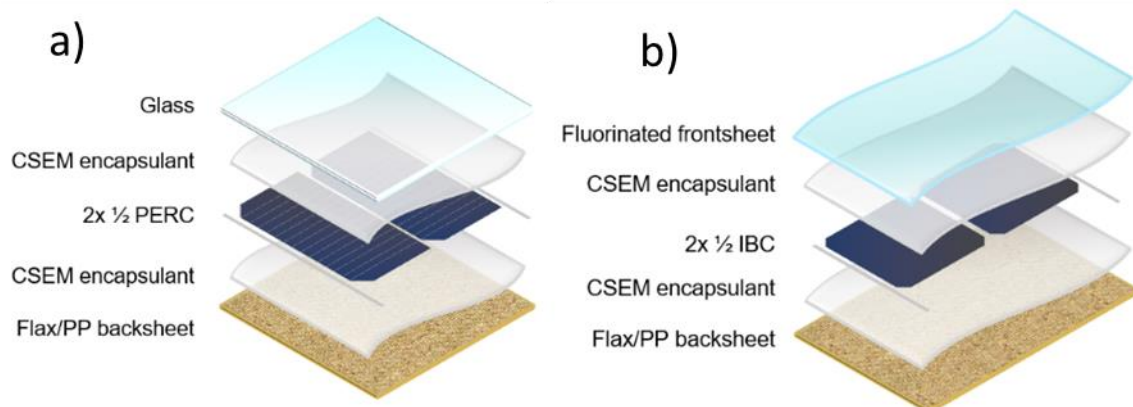


Figure 10 Schematic BoM of a) glass/backsheet modules with flax backsheet b) lightweight module with fluorinated frontsheet and flax backsheet

As shown in Table 4 mini modules present a good visual aspect without bubbles and do not show cracks after lamination in EL images.

Table 4 Visual inspection and EL images of the mini-modules with flax backsheet.

	Visual inspection	EL
Front glass module with flax backsheet		
Lightweight module with flax backsheet		

Light IV curves were performed to assess the performance of the mini modules. The results, shown in Figure 11, demonstrate the excellent performance of the optimized encapsulation process used for the flax backsheet.

It is noteworthy that the reference mini modules exhibited a higher I_{sc} . This could be attributed to the higher reflectivity of the commercial backsheet, which is white and includes an aluminium layer, leading to increased light collection inside the bifacial PERC solar cells compared to the flax backsheet.

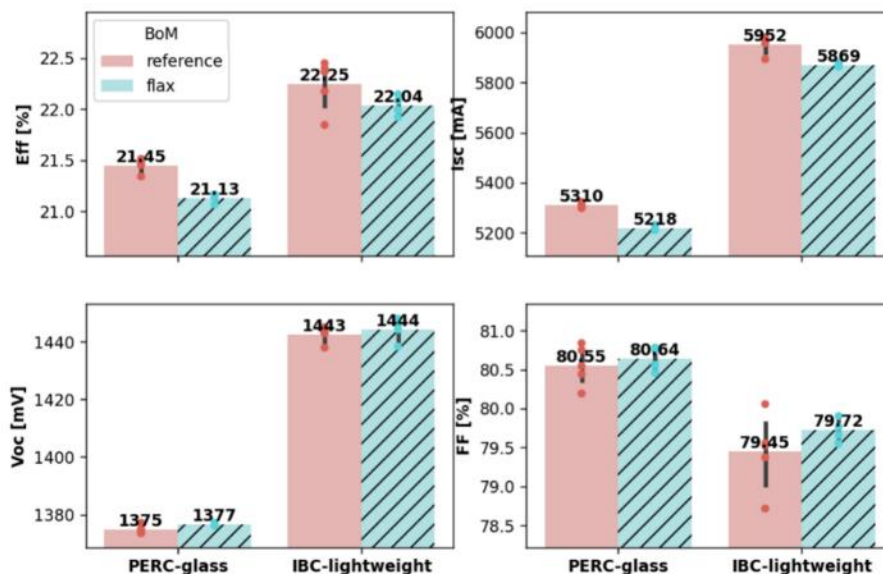


Figure 11 Performance of modules conventional flax backsheet in conventional and lightweight configurations

To evaluate their stability, the modules were tested under damp heat (DH) and thermal cycling (TC) conditions. DH testing is critical because flax fibres tend to absorb moisture, which can affect the mechanical performance of the composite. TC testing can lead to interconnection issues and cell cracking due to mismatches in the thermal expansion coefficients of the module materials.

Figure 12 shows that PERC modules fail in TC testing due to interconnection losses, while IBC lightweight modules remain very stable and achieve 1.5 times the IEC standard. Figure 13 demonstrates that all modules pass 2 times the IEC standard in DH testing, which is promising.

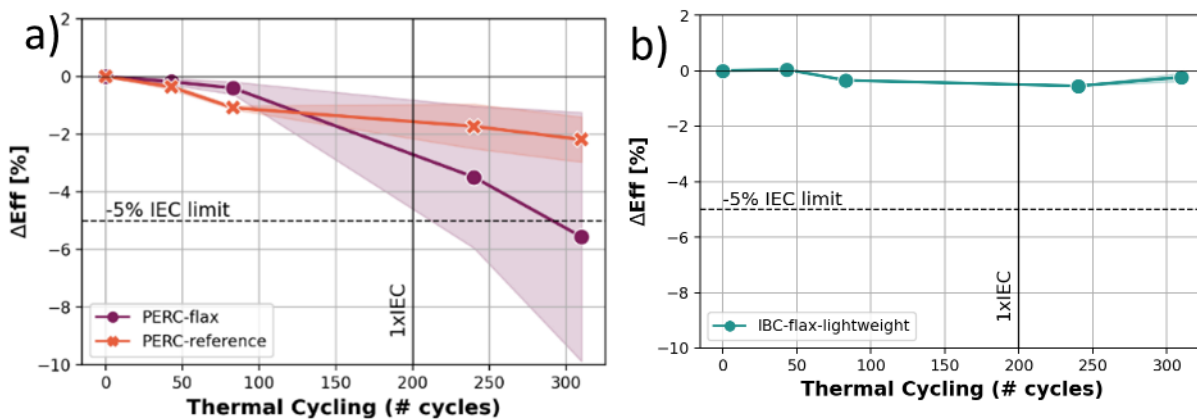


Figure 12 Efficiency losses of a) PERC flax and reference modules and b) IBC in thermal cycling

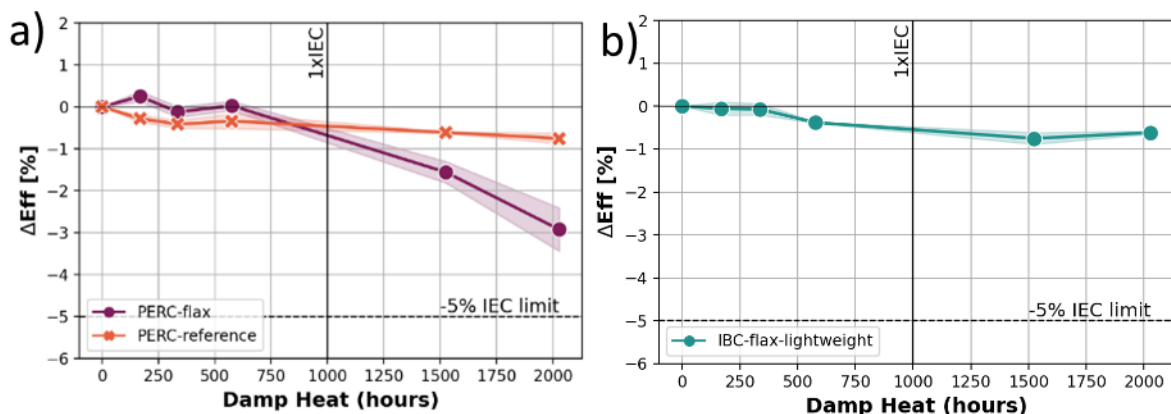


Figure 13 Efficiency losses of a) PERC flax and reference modules and b) IBC in damp heat

As a preliminary test, modules with wood backsheets were made. A 21 cells module was made (see Figure 14), the module passed 1xIEC in HF with only 0.7% performance loss.



Figure 14 Lightweight module with a wood backsheet

Improved BoM

In the previous section, lightweight modules with a fluorinated frontsheet or front glass, which are commercially available solutions, were presented. As discussed, the goal is to eliminate fluorine from the modules. Therefore, CSEM developed its own non-fluorinated frontsheet.

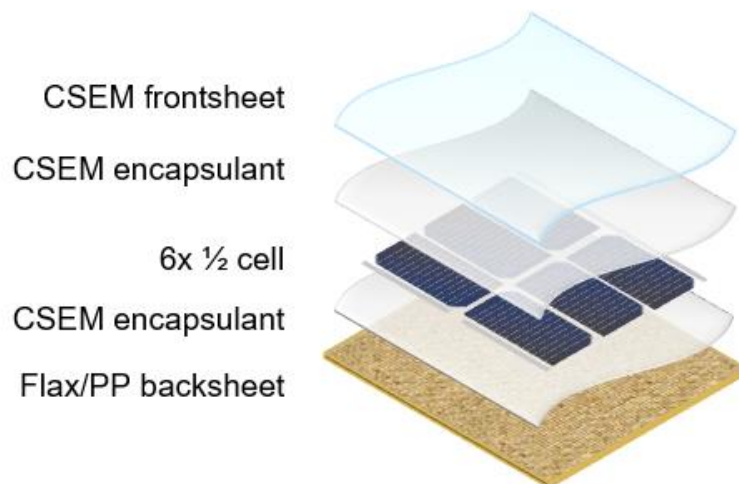


Figure 15 CSEM module stack with non-fluorinated frontsheet, CSEM encapsulant that can be biobased and a biobased composite backsheet

A new experiment was designed to test modules comprising the newly developed frontsheet, CSEM encapsulant, and flax backsheet. Additionally, three types of solar cells were tested: PERC, IBC, and SHJ with 0BB interconnection, which is the targeted cell technology in the RESILEX project.

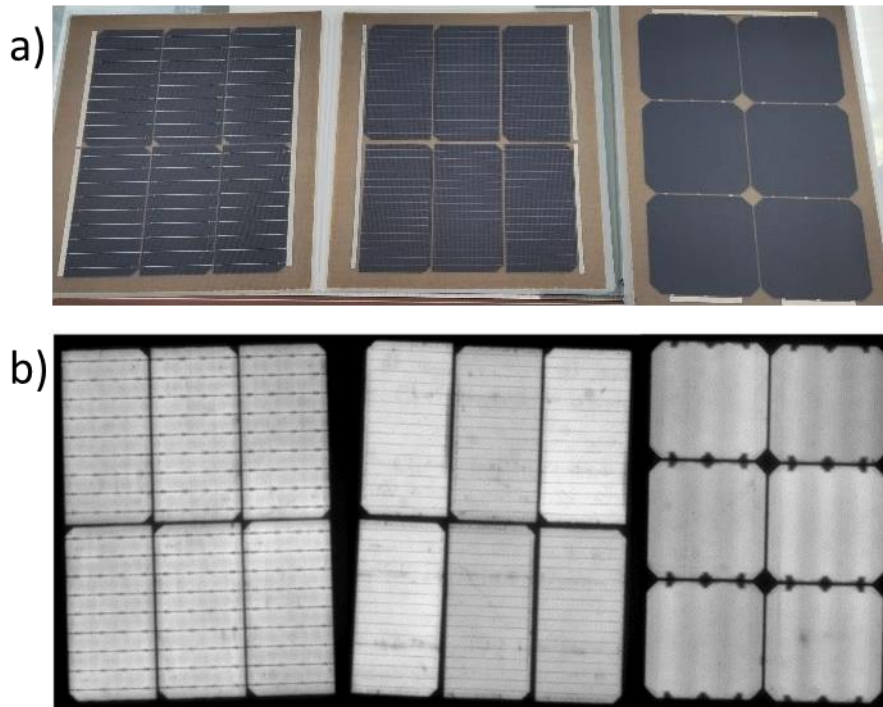


Figure 16 a) Image and b) EL of modules with, from left to right PERC, SHJ and IBC cells

As demonstrated in Figure 16, after lamination the modules do not show visual defects or cell breakage. The materials seem to be compatible with one another for lamination process.

The reliability of the modules under damp heat (DH) and thermal cycling (TC) conditions was evaluated. The interconnection losses in TC observed in the PERC cells from the previous experiment have been resolved. All modules demonstrated stability, achieving 2 times the IEC standard in TC testing. Unfortunately, the bill of Material chosen is not adapted for the used PERC cells, leading to performance loss.

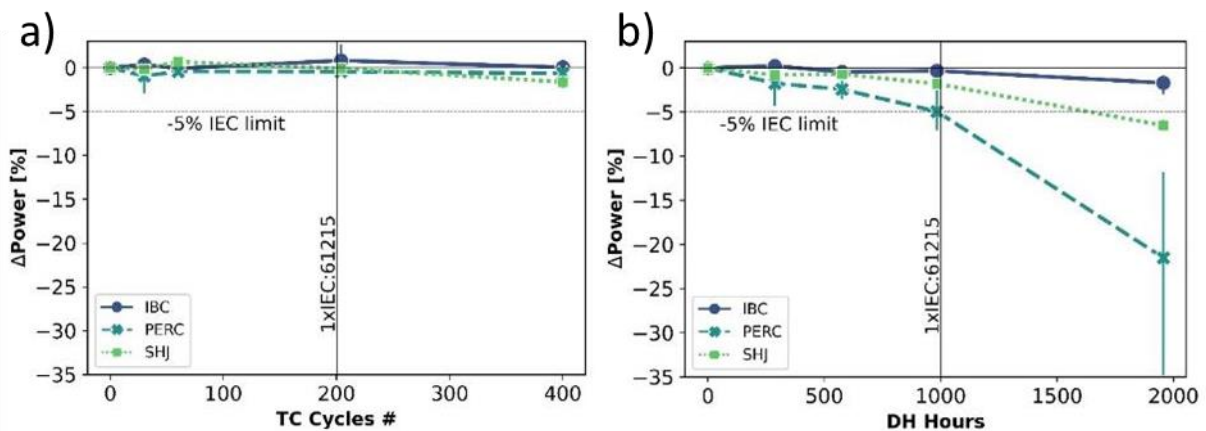


Figure 17: Power loss of modules after a) and b) DH for 2 times IEC

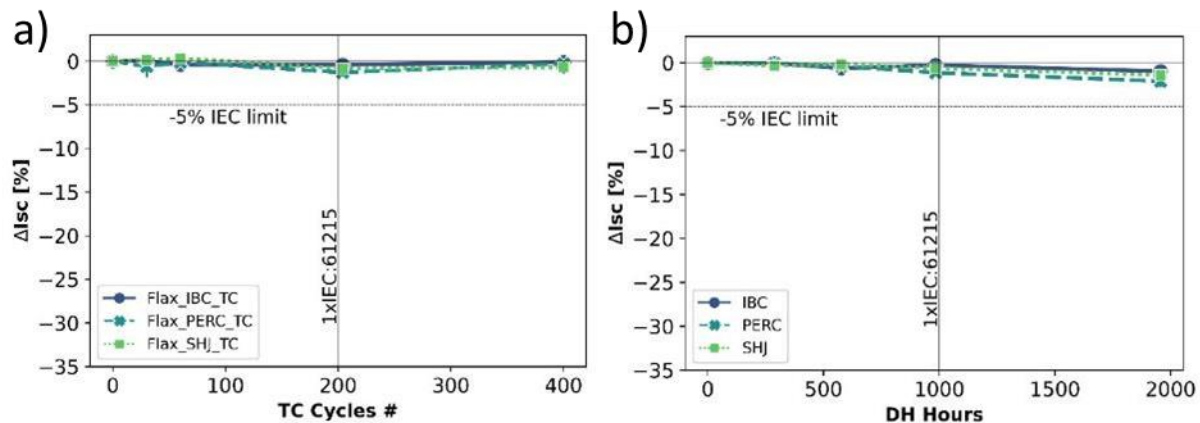


Figure 18 Isc losses after a) TC and b) DH

Figure 18 shows that the I_{sc} of all the tested modules are stable. It means that the transmittance of the backsheet and the encapsulant remain stable.

We are currently calculating the LCA of these modules.

One of the challenges in frontsheet development is ensuring safety. IEC Standard 62788 outlines various elements that must be assessed, including breakdown voltage, thermal endurance, and insulation properties. These measurements are currently being conducted.

4.5 CEA: biobased materials implementation in modules

4.5.1 First testing campaign

Previously tested project encapsulants (CSEM TPO and CSEM TPOUV) with validated BOM had been integrated in mono-modules of two interconnected SHJ half cells. We fabricated ten modules with glass / glass (G) or glass / backsheet (BS) configuration. We used project's SHJ solar cells with reduced silver and indium content in the transparent conductive oxide (TCO) layer. Figure 19 presents the used cell architecture. The main steps of this campaign were as follows:

- (Possibly) bio based encapsulant (CSEM TPO and CSEM TPOUV) laminated in classic BOM configuration (G or BS) compared to commercial encapsulant TPO2 in BS configuration
- Initial performance measurements (Flash test + EL)
- Accelerated aging had been launched for 3000 h with intermediate measurement steps at 250 h, 500 h, 1000 h.

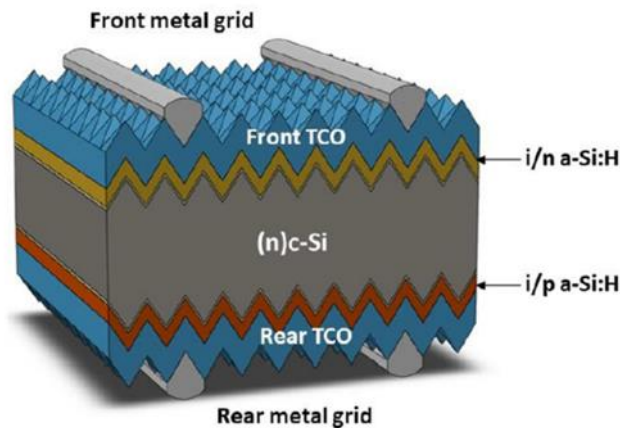


Figure 19 SHJ cell structure used for damp heat aging

The used Ag-less and In-less SHJ solar cells had the following specifications:

- SHJ solar cells encapsulated: M2 SHJ half cells with 18 busbars
- Metallisation: Screen-printing of silver coated copper particles pastes (Ag/Cu) with Ag consumption reduced by 50 to 60% compared to standard SHJ
- TCO: Test of 2 ITO thicknesses: 100 nm (reference) and 30 nm (corresponding to In reduction of 70%)
- ECA interconnection

Initial module performance

Table 5 shows the ten manufactured modules' BOM.

Table 5 Module bill-of-material (BOM)

		Frontsheet	Encapsulant (front/rear)	SHJ cell ITO thickness (nm)	Rear face
1	CSEM TPO_ITO30_BS	Glass	CSEM TPO	30	Polymer
2	CSEM TPO_ITO30_G	Glass	CSEM TPO	30	Glass
3	CSEM TPOUV_ITO30_G	Glass	CSEM TPOUV	30	Glass
4	CSEM TPO_BS	Glass	CSEM TPO	100	Polymer
5	CSEM TPOUV_ITO30_BS	Glass	CSEM TPOUV	30	Polymer
6	CSEM TPOUV_BS	Glass	CSEM TPOUV	100	Polymer
7	CSEM TPO_G	Glass	CSEM TPO	100	Glass
8	CSEM TPOUV_G	Glass	CSEM TPOUV	100	Glass
9	TPO2_ITO30_BS	Glass	commercial	30	Polymer
10	TPO2_BS	Glass	commercial	100	Polymer

We measured initial module performance right after lamination. Figure 20 presents the electrical performance of the ten studied modules. At T0 thicker ITO layered cells seem to have better initial Pmax performance. TPO2 modules correspond to modules made with a commercially available, partially bio-based polymer encapsulant with the same backsheet as other modules of the campaign (reference modules). Figure 21 presents electroluminescence (EL) images of the ten studied modules at T0. No cracks or other defaults are present. Therefore, we sent all the modules in damp heat aging in

accordance with standard 61215 - 1:2021[15]. The ten modules were exposed to 3000 h of DH, first with steps of 250 h, then 500 h and finally 1000 h for intermediate measurements.

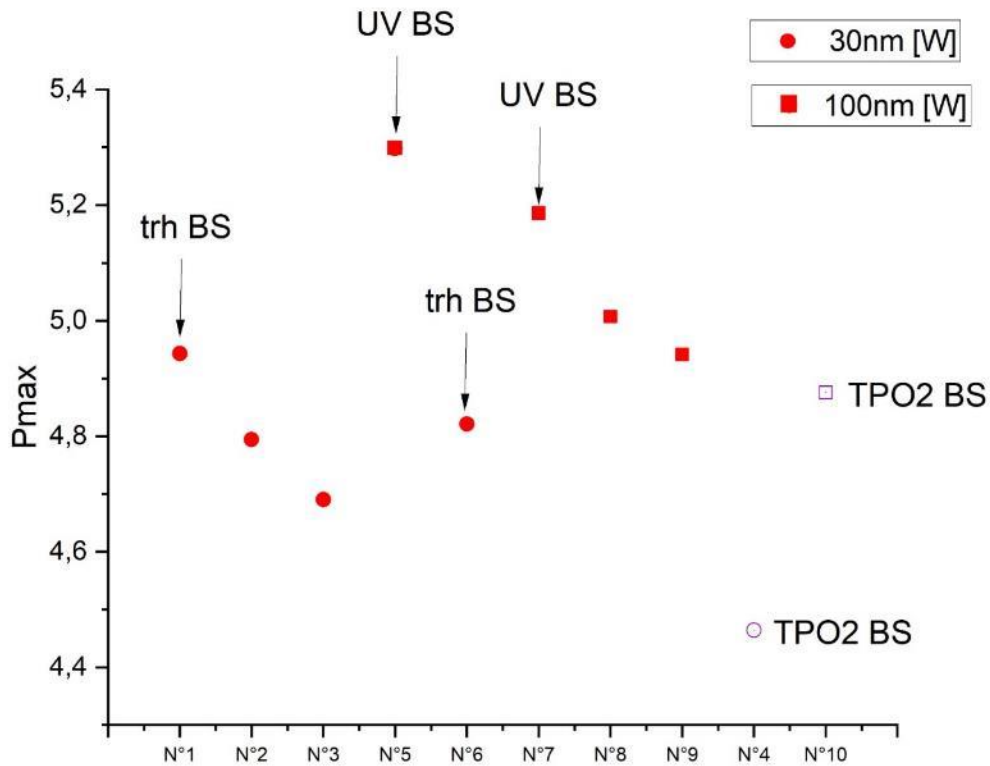


Figure 20 Initial Pmax values of ten mono modules described in table 5.

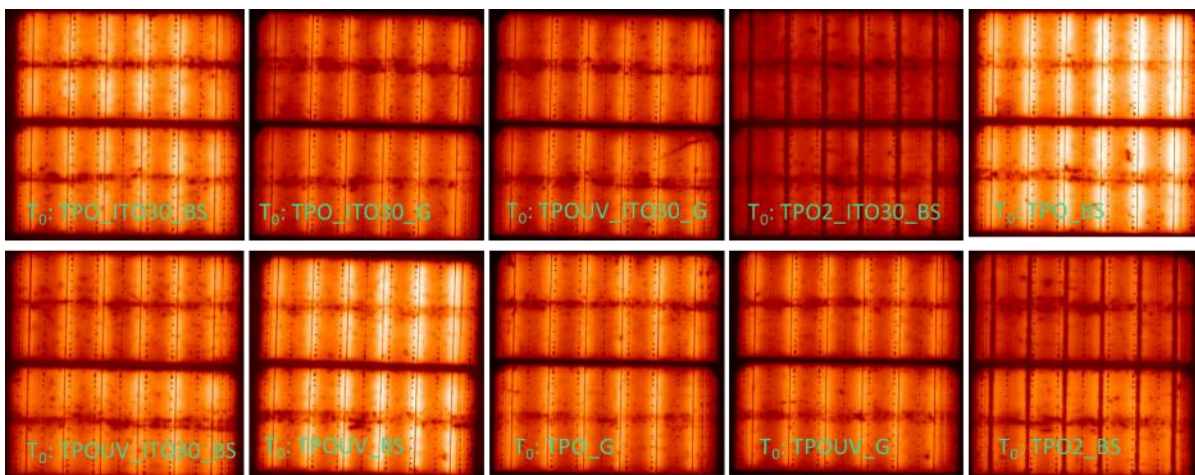


Figure 21 Initial electroluminescence images of the ten studied mono modules

Electric performance in aging

Figure 22 shows the maximum power variation during aging of the studied modules made with thin ITO layer. The most striking result of this experimental campaign is the fact that all the studied modules passed the 1,5 x times the standard criterion in DH exposure. This is reflected in the fact that after 1500 h of DH, the modules lost less than 5 % of their maximum power compared with their initial performance. After 3000 h (3 x

times) of DH all modules had Pmax variation over 5 %, allowed by the standard at 1 x time. Worst performance, largely below the GBs version, had been obtained for TPO GG module with thin ITO layer. Best performance belongs to TPO2 module.

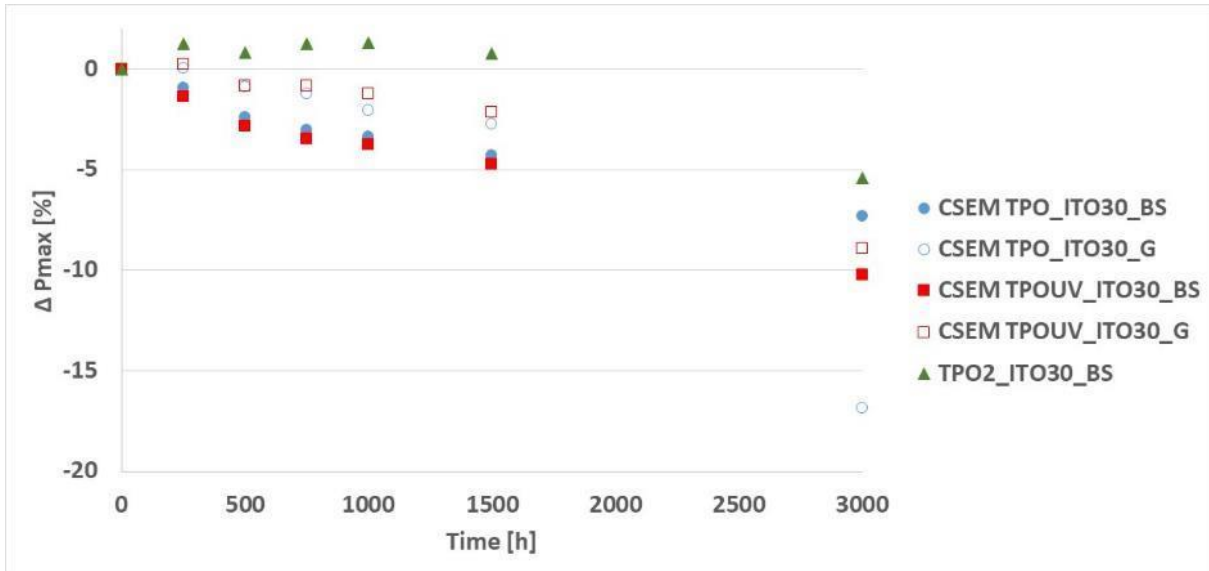


Figure 22 Variation in maximum module power output (Pmax) during DH aging - Cells with thin ITO

Figure 23 presents Pmax variation for thick ITO layered modules in DH. As for thin version, all modules had passed 1,5 x times the modules requirement (< 5 % Pmax loss). Two modules even had passed 3 x times the standard's requirement which is a very good result for this first trial. We noticed more than 10 % gap between versions GG and GBs of TPO made modules and once again it is the GG version of this encapsulant that had the worst electric performance at 3 x times the standard.

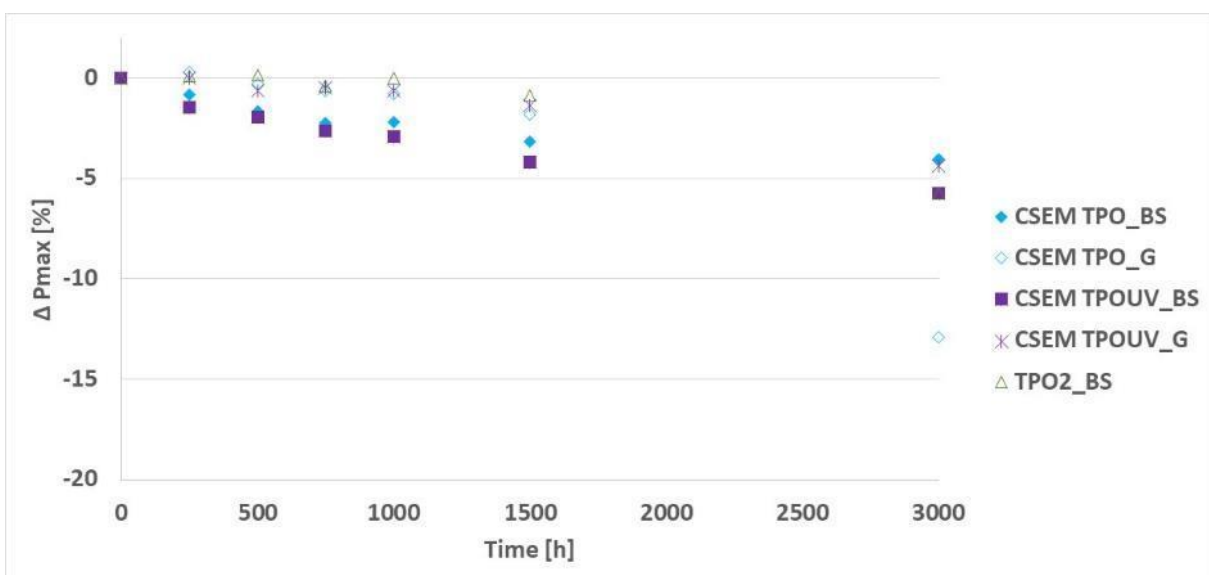


Figure 23 Variation in maximum module power output (Pmax) during DH aging - Cells with thick ITO

To understand the loss of performance Figure 24 and Figure 25 present short circuit current (Isc) and fill factor (FF) values of the studied modules. Worst performing

modules (TPO G and TPO_ITO30_G modules have the worst I_{sc} performance while TPO_ITO30_G module has also the worst FF performance simultaneously).

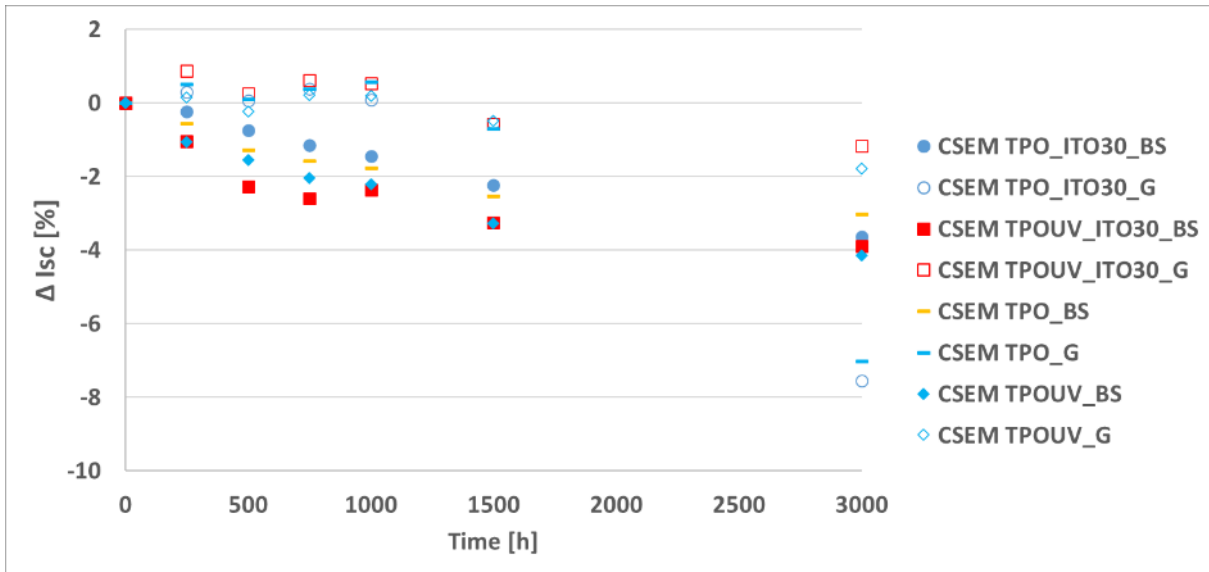


Figure 24 Variation in short circuit current (I_{sc}) during DH aging - Cells with 2 different ITO thicknesses

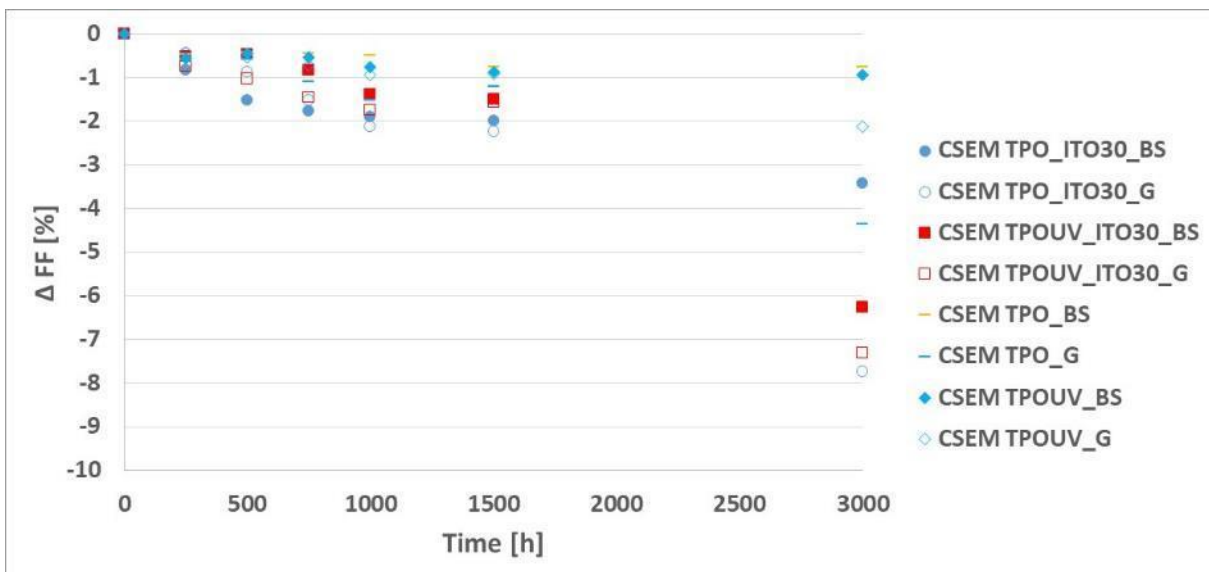


Figure 25 Variation in fill factor (FF) during DH aging - Cells with 2 different ITO thicknesses

I_{sc} losses are not correlated to ITO thickness, no main pattern had been identified while for FF losses we noticed a strong link with thin ITO thicknesses.

Figure 26 shows EL images of the ten tested modules after 3000 h of damp heat exposure. Modules made with the same encapsulant (TPO) in glass / glass configuration (the CSEM TPO_ITO30_G module is made with cells with an ITO thickness of 30 nm and the CSEM TPO_G module is made with cells with an ITO thickness of 100 nm) shows the most important degradation patterns. After 3000 h of exposure, we note a darkening of the central areas of the modules between the interconnections. This same effect is present also in module CSEM TPOUV_G and CSEM TPOUV_ITO30_G

but in a less important level (in all tested GG configuration modules). This suggests that the moisture may have affected the cells across their entire surface, and not just at the edges as expected in the glass / glass configuration. Pirot-Berson et al. suggested that this kind of degradation pattern may be related to glass lixiviation under sodium ion migration [28]. As a matter of fact, this degradation profile is not present with GBs configuration as showed in Figure 26. Another degradation pattern had been identified on modules made with TPO2 encapsulant. These modules, independently from ITO thickness, showed a darkening under bus bars. After visual inspection a delamination was identified as shown in Figure 27. To confirm the delamination, we observed the zone under 20 magnifications by an optical microscope (Keyence). Figure 28 shows the delamination of the encapsulant from the cell following an inter - finger texture. The delaminated zones increased with the DH testing progression.

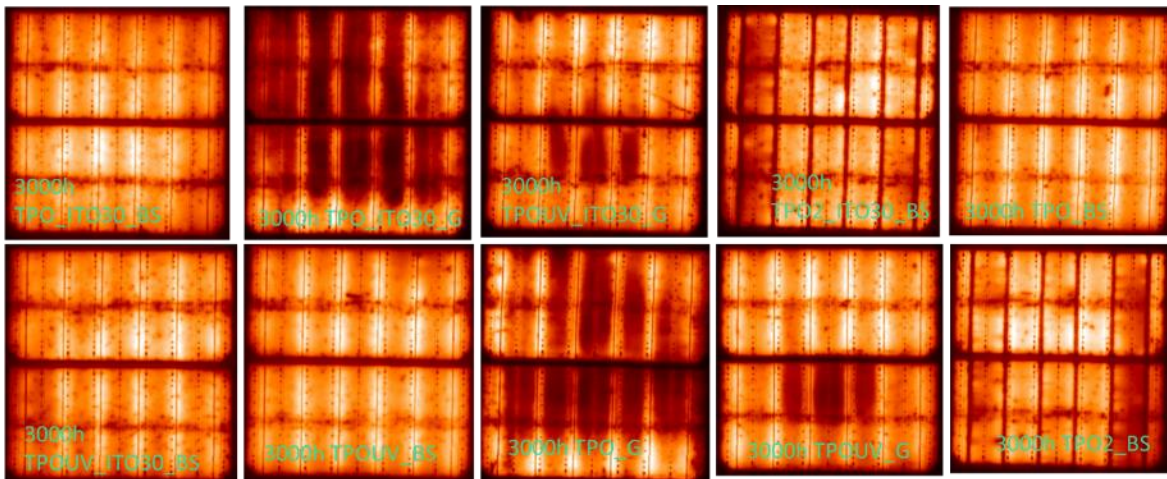


Figure 26 EL images of the ten studied modules at 3000h of damp-heat aging

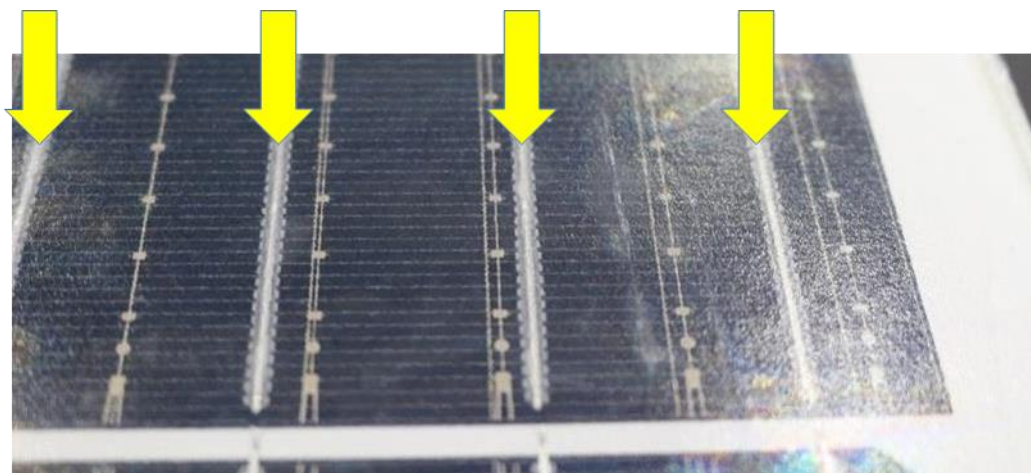


Figure 27 TPO2 module at intermediate measurement during DH aging

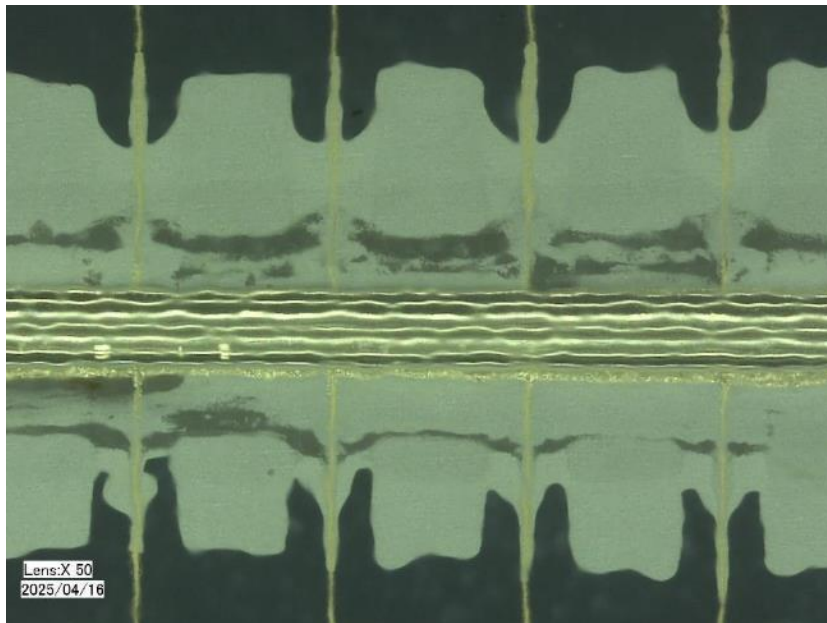


Figure 28 Optical microscope image of the delaminated interconnection on TPO2 module (TPO_IT030_BS)

This delamination phenomena could be attributed to interconnection process.

Conclusions of first testing campaign

During this study we found that ITO thickness of 30 nm instead of 100 nm has no major influence on Pmax variation in DH aging up to 3000 h. Meanwhile, a slightly better Pmax performance belongs to thick ITO modules. 70 % of the studied modules passed the damp-heat aging standard 1,5 times (< 5 % Pmax loss after 1500 h DH) with European encapsulant and copper-based electrodes and 30% of the studied modules passed the damp-heat aging standard three times. Best aging performance belongs to modules made with CSEM TPO encapsulant using SHJ cells with copper-based electrodes. The impact of the glass / backsheets configuration was also analysed for the two encapsulants in the project (CSEM TPO and CSEM TPOUV). Contrary to expectations, the glass/glass modules lost more power after 3000 h than the glass/backsheets modules with CSEM TPO encapsulant for both ITO thicknesses. It may come from premature cell degradation or glass leaching. This tendency was not recorded for CSEM TPOUV encapsulant made modules.

4.5.2 Second testing campaign: integration of a bio-based polymer frontsheet

This second experimental campaign concerns the integration of an experimental bio-based polymer frontsheet in mono module configuration with two half cells. Full polymer modules, containing different polymers at front and rear side, requires careful manufacturing process to avoid unwanted curving. In consequence, we started the lamination optimisation with polymer sheets alone, without solar cells. For this campaign we used

- A full bio-sourced polymer frontsheet (experimental version, not yet available on market),
- Partly bio-based encapsulant (on market)
- Fluorine free EU backsheets with third part recycled PET (on market).

First tests suggested to use an initial lamination step to release intrinsic constraints in polymer. In second step we obtained less curving but cell breaks as showed in Figure 29 (a). It may come from laminator pin impact thus we adopted the lamination process to protect modules. Final version has no cell break. We decided to send these two modules (Figure 29 (b)) to thermal cycling aging as it is a crucial point of full polymer modules reliability analysis.

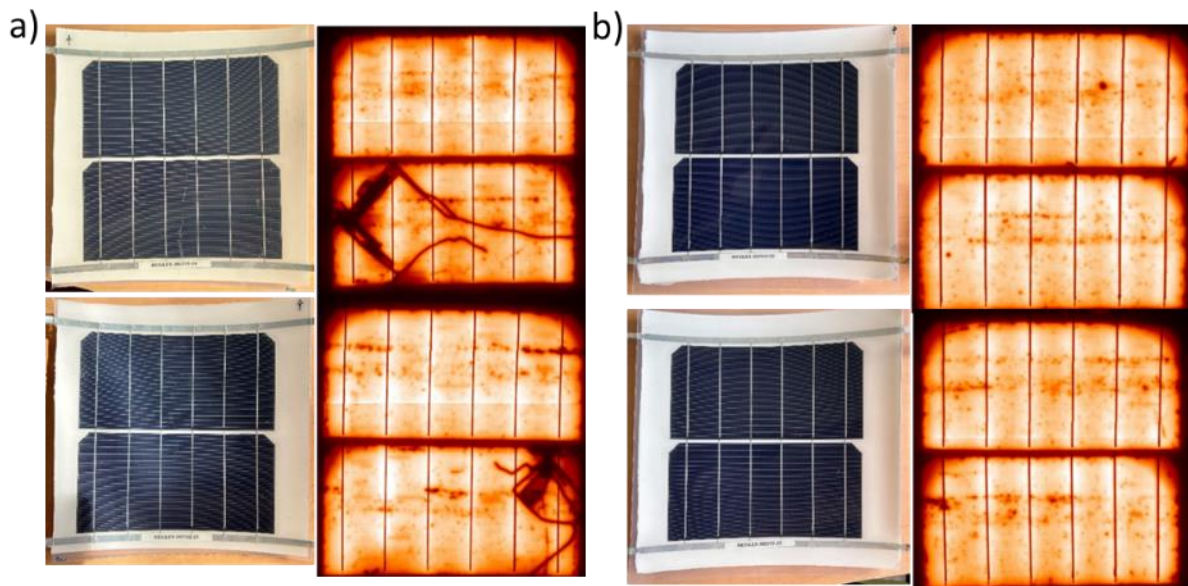


Figure 29 Lamination trials with polymer stack a) second trial with broken cells b) third trial with ameliorated lamination process with no cell break

Figure 30 shows the EL images of the four modules that were sent to thermal cycling aging. After 50 cycles of thermal cycling, we discarded both modules of the second trial, those which presented already cell breaks. The two modules of the third trial were sent for further TC testing and will be presented in the final deliverable of the work package.

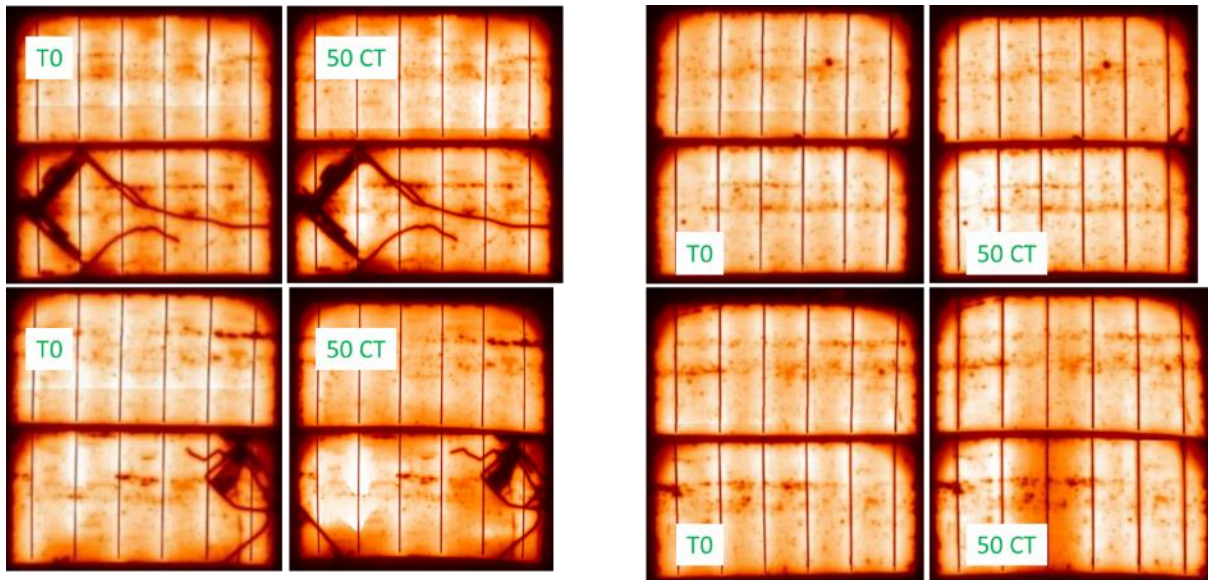


Figure 30 EL images at initial and at 50 TC aging of the four modules

This trial enables us to continue with further testing of this frontsheet by upscaling the BOM to 2x4 half-cells configuration. This study will be included into the final version of this deliverable as a joint experiment between CEA and CSEM.

4.5.3 Frame

The global annual production of photovoltaic (PV) modules is growing rapidly. For efficiency reasons, these modules are becoming increasingly larger and thinner, often using glass/backsheet architectures, which reduces their mechanical stability. In this context, the frame, which reinforces the panel, plays a crucial role. For a typical glass/backsheet module, the frame accounts for 10% of the cost and 12% of the total carbon footprint. Our goal is to develop a model that allows for comparing the mechanical stability of modules based on the type of frame used.

Methodology

Our initial objective was to characterize the bending strength—and thus the flexural modulus—of four different aluminium frame references, in order to understand its influence on the results of the SML static load test for modules.

To achieve this, we performed four-point bending tests on short-side samples from each of the frame references to be tested. It's important to note that the tested frames have profiles with different geometries on the long and short sides. However, the difference in flexural modulus between the short-side and long-side profiles was found to be very small (1.2%), and is therefore considered negligible. Three identical short-side samples were tested for each frame reference. Subsequently, a test module was manufactured for each frame reference and subjected to a static pressure of

+2400 Pa and -2400 Pa, in accordance with the SML test protocol described in the IEC 61215 standard. The mounting system used consisted of four clamps holding the frame on its long sides at 20 % and 80 % of the module height. The pressure levels of +2400 Pa and -2400 Pa correspond to the minimum required to pass the standard test. In our case, to simplify the approach, we focused solely on the static response of the module. Therefore, we applied one-minute loading and one-minute holding intervals. Only one cycle of positive and negative pressure was performed per test.

Finally, using Abaqus software, we developed a finite element simulation model to represent the deformation and stress state of a module subjected to the test previously described. To begin with, we created a simplified model representing the cell matrix as a single uniform silicon layer matching the laminate's dimensions. The laminate was first modelled with a boundary condition representing four clamps holding the laminate without a frame, and then modelled with a fully fixed boundary condition on its perimeter, simulating a perfectly rigid frame as showed in Figure 31.

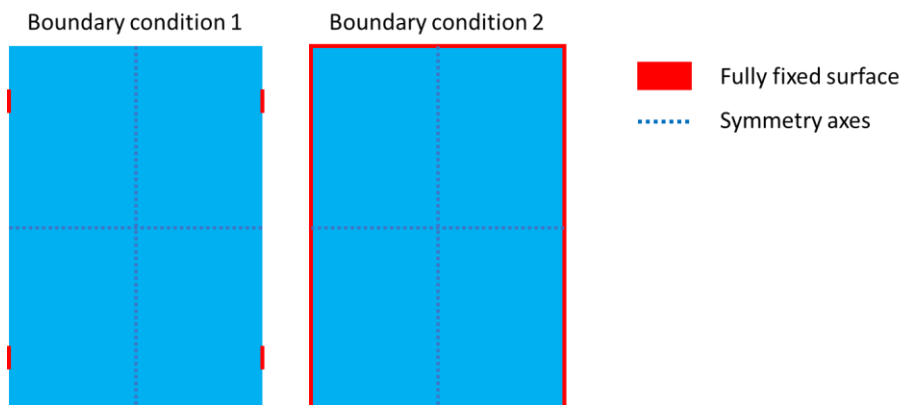


Figure 31 Both studied boundary conditions of the numerical study

Next, we developed a more detailed model using a Python script that generates a set of parallelepiped-shaped silicon cells. A reference aluminium frame was added to this model, and then compared with four different frame models made of black locust (robinia) wood.

Mesh optimisation:

Result of numerical simulation depends on mesh's quality. To obtain the optimal solution we need to find the adequate mesh elements' size and density (cf. Figure 32). We optimised the cell number for simulation by finding a compromise between precision and calculation time.

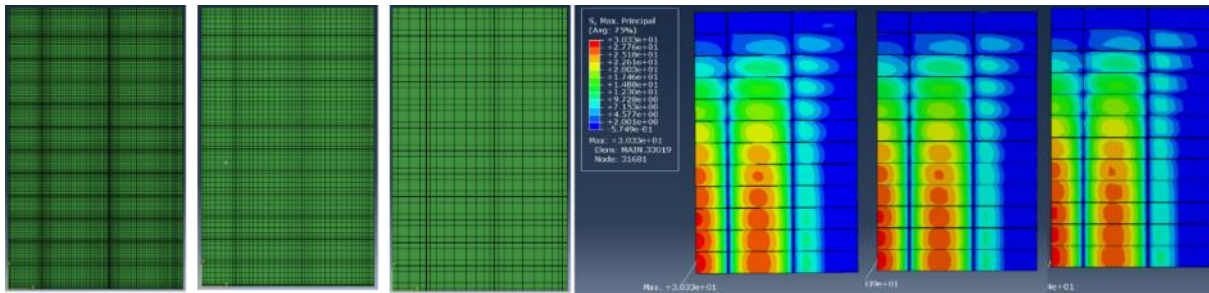


Figure 32 Mesh optimisation in three stages with associated strength results

Simulation results

Despite their very small thickness, it appears the cells play an important role in the overall stiffness of the laminate. It is therefore crucial to model them accurately in order to obtain representative stress and deformation levels. The maximum stress level in the cells and in the glass is lower when the laminate is embedded in a rigid frame compared to when it is held by the four standard mounting clamps. The frame thus effectively reduces the laminate's deflection and internal stresses. Under a pressure of +2400 Pa, the central deflection of the module remains nearly constant across all four aluminium frames tested. We can conclude that there is no correlation between the central deflection of the laminate and the flexural modulus of the frame used. Under a pressure of -2400 Pa, we observe that the deflection decreases as the flexural modulus of the frame increases. The stress level is consistently higher—and closer to the material's failure threshold—in the glass than in the cells. Therefore, the greatest risk of failure lies in the glass. The situation in which internal stresses are the highest is during the positive pressure test at +2400 Pa, with the maximum stress in the glass occurring at the clamp holding the frame (cf. Figure 33).

It is possible to reduce the maximum stress level in the glass by increasing the thickness of the silicone seal used between the laminate and the frame, or by adding a hinge-like connection between the frame and its support at the clamp location. In such cases, the laminate's deflection and the stress level in the cells increase slightly. According to our models, it is theoretically possible to achieve similar mechanical performance by replacing the aluminium frame with one made of local wood species. However, this alternative would necessarily be heavier for equivalent performance (approximately 35 % increase in weight).

Wood is more difficult to predict and model than aluminium. While its orthotropic properties can be modelled, its non-homogeneous nature is more challenging to represent. Wood contains knots and its fibres are not always perfectly aligned. In our four-point bending tests, we observed that the thinnest wood profiles we considered (outer dimensions 30 × 20 mm) can break during the test well before reaching their

theoretical maximum flexural stress. In such cases, failure consistently occurs near a knot in the wood as showed in Figure 34.

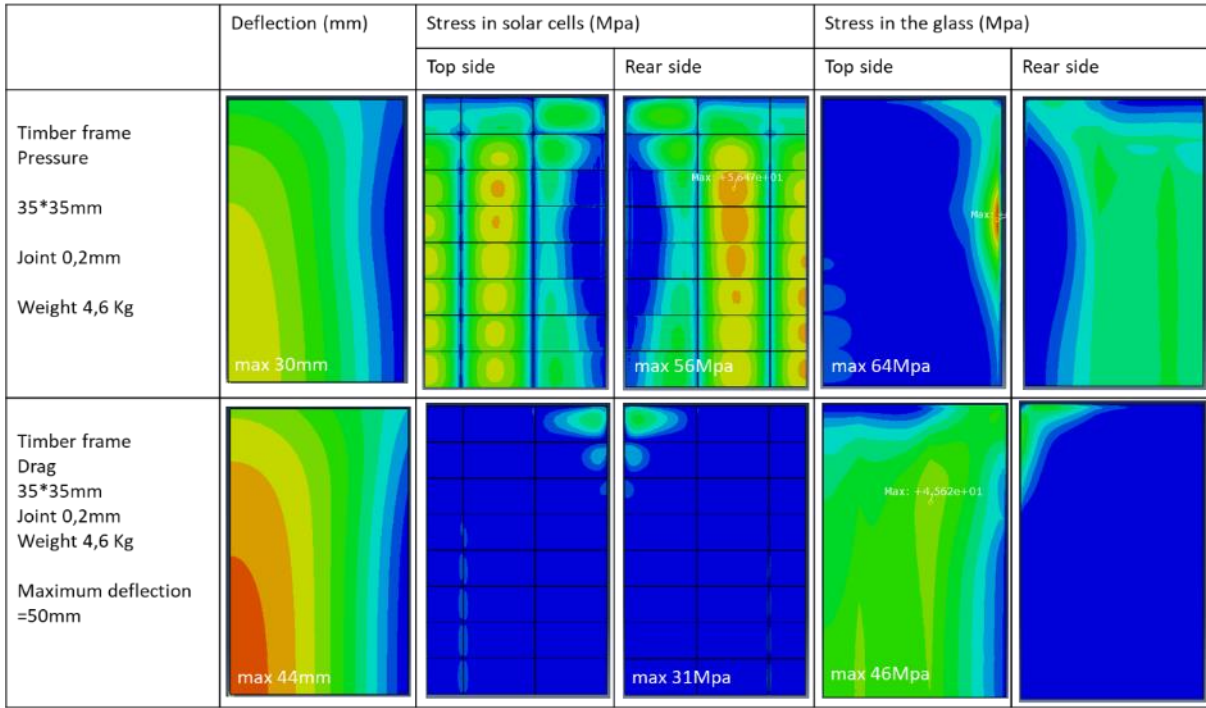


Figure 33 Simulation results of central deflection, max level of stress in cells and in glass



Figure 34 Wood knot where cracks form systematically

In order to assess these numerical results, the final module with wood frame should undergo IEC61215 standard's mechanical testing sequence. Static mechanical loading (SML) test covers 5400 Pa loading homogenously on a PV module at initial stage and after

- 200 thermal cycles (-40 °C to 85 °C), or
- 10 cycles of humidity / freeze.

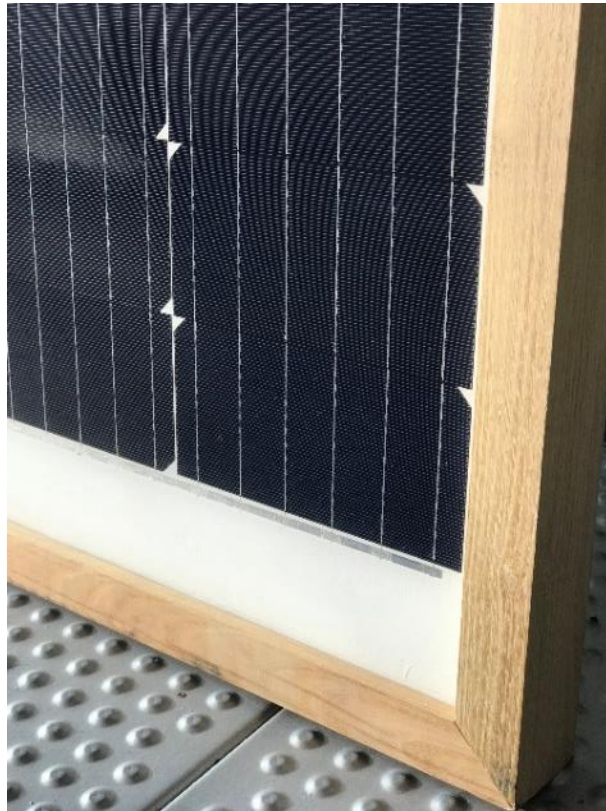


Figure 35: Finalized wooden frame

Figure 35 presents the final display of the wooden frame of a PV module. This module can be tested then in damp heat conditions also. These tests are not the most critical tests for wood, thus degradation due to the substitution of aluminium by wood as frame material should not affect damp heat performance of the full module [22], [28].

5 Conclusions

In a first section we conducted a literature review on the use of biobased materials in PV modules. The review revealed that much of the existing literature focuses on replacing polymeric backsheet with bio-based composites. However, there are fewer examples of substituting fossil-based with bio-based alternatives. Additionally, some studies lacked reliability testing for modules containing biobased materials. Notably, replacing aluminium frames with wooden frames showed significant potential to reduce the carbon emissions associated with PV module manufacturing.

We proposed a methodology for selecting biobased materials PV modules which includes material screening, testing and implementation at the module level. We also recommend conducting an LCA to ensure environmental benefit at module level. Additionally, we discussed the environmental aspects related to the use of biobased materials. At material level, the environmental benefits of biobased materials are not

always guaranteed. Furthermore, substituting materials does not necessarily result in a lower impact on electricity production as it depends on the performance and the lifespan of the module. Therefore, all these factors must be considered when making material choices.

We also have performed, experimental work. We have formulated and incorporated two versions of a European encapsulant into photovoltaic modules. This first experiment enabled us to validate the two encapsulants (one that cuts UV radiation and one that lets it through), using solar cells with reduced amount of Silver and Indium, and for two module configurations: glass / glass and glass / backsheet (size 20 cm x 20 cm). Initial aging tests have been very encouraging, with all modules passing the standard IEC standard requirement (less than 5 % Pmax loss after 1000 h in damp heat at 85 °C and 85 % relative humidity) 1,5 times (1500 h DH). We now need to explore the various degradation mechanisms of our modules to improve them before next test campaigns.

We also have formulated a fluorine-free frontsheet and combined it with natural flax fibres /PP backsheet to make modules. The modules that either had, PERC, IBC or SHJ cells showed good reliability in TC and DH, two critical conditions. As next steps we will evaluate the safety of the developed frontsheet.

The objective of frame study, through finite element modelling, was to analyse the feasibility of replacing existing PV module frames with an eco-designed alternative that has a reduced carbon footprint. To this end, we conducted four-point bending tests as well as mechanical bench tests based on the SML test from the IEC 61215 standard. In parallel, we developed a numerical model representing a typical glass/backsheets module with its frame subjected to the SML test. This allowed us to compare the stress levels in the cells, in the glass laminate, and in the different frame models studied. We found that the stress level is consistently higher—and closer to the material's failure threshold—in the glass than in the cells. Therefore, the greatest risk of failure lies in the glass. The situation in which internal stresses are the highest is during the positive pressure test at +2400 Pa, with the maximum stress in the glass occurring at the clamp holding the frame. As a next step we will explore timber framed full size module behaviour in SML testing and continue to explore the market to acquire alternative frames to aluminium such as composites.

6 References

- [1] 'Global Solar Council announces 2 terawatt milestone achieved for solar', Global Solar Council. Accessed: Apr. 24, 2025. [Online]. Available:

- <http://www.globalsolarcouncil.org/news/global-solar-council-announces-2-terawatt-milestone-achieved-for-solar/>
- [2] A. Müller, L. Friedrich, C. Reichel, S. Herceg, M. Mittag, and D. H. Neuhaus, 'A comparative life cycle assessment of silicon PV modules: Impact of module design, manufacturing location and inventory', *Solar Energy Materials and Solar Cells*, vol. 230, p. 111277, Sep. 2021, doi: 10.1016/j.solmat.2021.111277.
 - [3] M. Fischer, M. Woodhouse, and P. Baliozian, 'International Technology Roadmap for Photovoltaics (ITRPV) 2023 results', VDMA e. V. Photovoltaic Equipments, Frankfurt, 2024.
 - [4] Shravan Kumar Chunduri and M. Schmela, 'Market Survey Backsheets and Encapsulation 2022-2023', 2023, doi: 10.13140/RG.2.2.11206.45124.
 - [5] K. Miettunen *et al.*, 'Bio-based materials for solar cells', *WIREs Energy & Environment*, vol. 13, no. 1, Art. no. 1, Jan. 2024, doi: 10.1002/wene.508.
 - [6] S. Agarwal, 'Biodegradable Polymers: Present Opportunities and Challenges in Providing a Microplastic-Free Environment', *Macro Chemistry & Physics*, vol. 221, no. 6, p. 2000017, Mar. 2020, doi: 10.1002/macp.202000017.
 - [7] A. Z. Naser, I. Deiab, and B. M. Darras, 'Poly(lactic acid) (PLA) and polyhydroxyalkanoates (PHAs), green alternatives to petroleum-based plastics: a review', *RSC Adv.*, vol. 11, no. 28, Art. no. 28, 2021, doi: 10.1039/D1RA02390J.
 - [8] M. Zulkeply, M. M. Pang, C. A. Vaithilingam, and R. Sivasubramanian, 'The fundamental studies on the reaction kinetics of thermal decomposition of bio-composite based backsheet materials in photovoltaic (PV) panel', *J. Phys.: Conf. Ser.*, vol. 2222, no. 1, Art. no. 1, May 2022, doi: 10.1088/1742-6596/2222/1/012002.
 - [9] S. B. Levy, 'Bio-based backsheet', presented at the Solar Energy + Applications, N. G. Dhere, Ed., San Diego, CA, Aug. 2008, p. 70480C. doi: 10.1117/12.792646.
 - [10] M. Pander, R. Koepge, B. Jaeckel, and A. Mordvinkin, 'Material Screening for the Development of Photovoltaic module Usin Biodegradable Materials from Renewable Raw Materials', presented at the EUPVSEC2024, Wien, AUT, 2024.
 - [11] S. B. Levy, 'Biobased PV backsheet', in *2011 37th IEEE Photovoltaic Specialists Conference*, Seattle, WA, USA: IEEE, Jun. 2011, pp. 003185-003188. doi: 10.1109/PVSC.2011.6186617.
 - [12] K. Resh-Fauster and G. Oreski, 'Biogene Kunststoffe für solartechnische Applikationen: Endbericht', Wien, AUT, 2014.
 - [13] R. Koepge, M. Pander, A. Mordvinkin, and S. Großer, 'Steps Towards a 100% Renewable Material Solar Module: Evaluating Material Substitutions for Encapsulation and Interconnection', presented at the EU PVSEC 2024, Wien, AUT, 2024.
 - [14] G. C. Eder *et al.*, 'Error analysis of aged modules with cracked polyamide backsheets', *Solar Energy Materials and Solar Cells*, vol. 203, p. 110194, Dec. 2019, doi: 10.1016/j.solmat.2019.110194.
 - [15] *IEC 61215:2021 Series, "Terrestrial photovoltaic (PV) modules—Design qualification and type approval"*, Technical Specification, Geneva., 2021.
 - [16] *IEC 61730:2023 Parts 1 and 2, "Photovoltaic (PV) module safety qualification"*, Geneva., 2023.
 - [17] M. H. Alaaeddin, S. M. Sapuan, M. Y. M. Zuhri, E. S. Zainudin, and F. M. AL-Oqla, 'Development of Photovoltaic Module with Fabricated and Evaluated Novel

- Backsheet-Based Biocomposite Materials', *Materials*, vol. 12, no. 18, Art. no. 18, Sep. 2019, doi: 10.3390/ma12183007.
- [18] M. H. Alaaeddin, S. M. Sapuan, M. Y. M. Zuhri, E. S. Zainudin, and F. M. Al- Oqla, 'Lightweight and Durable PVDF-SSPF Composites for Photovoltaics Backsheet Applications: Thermal, Optical and Technical Properties', *Materials*, vol. 12, no. 13, Art. no. 13, Jun. 2019, doi: 10.3390/ma12132104.
- [19] F. M. AL-Oqla and O. Fares, 'Investigating the effect of green composite back sheet materials on solar panel output voltage harvesting for better sustainable energy performance', *Energy Harvesting and Systems*, vol. 11, no. 1, Art. no. 1, Jan. 2024, doi: 10.1515/ehs-2023-0041.
- [20] G. Oreski *et al.*, 'Properties and degradation behaviour of polyolefin encapsulants for photovoltaic modules', *Progress in Photovoltaics*, vol. 28, no. 12, pp. 1277–1288, Dec. 2020, doi: 10.1002/pip.3323.
- [21] J. Singh, A. Kumar, A. Jaiswal, S. Suman, and R. P. Jaiswal, 'Luminescent down-shifting natural dyes to enhance photovoltaic efficiency of multicrystalline silicon solar module', *Solar Energy*, vol. 206, pp. 353–364, Aug. 2020, doi: 10.1016/j.solener.2020.05.067.
- [22] T. Singer, 'Wooden Photovoltaic Module Frames : Proof of Concept, Life Cycle Assessment and Cost Analysis', 2021. Accessed: Dec. 11, 2024. [Online]. Available: <https://urn.kb.se/resolve?urn=urn:nbn:se:uu:diva-454318>
- [23] T. Béjat *et al.*, 'Design for the environment: SHJ module with ultra-low carbon footprint', *Progress in Photovoltaics*, p. pip.3803, Apr. 2024, doi: 10.1002/pip.3803.
- [24] S. Walker and R. Rothman, 'Life cycle assessment of bio-based and fossil-based plastic: A review', *Journal of Cleaner Production*, vol. 261, p. 121158, Jul. 2020, doi: 10.1016/j.jclepro.2020.121158.
- [25] B. P. Chang, A. K. Mohanty, and M. Misra, 'Studies on durability of sustainable biobased composites: a review', *RSC Adv.*, vol. 10, no. 31, pp. 17955–17999, 2020, doi: 10.1039/C9RA09554C.
- [26] M. Ramesh, C. Deepa, L. R. Kumar, M. Sanjay, and S. Siengchin, 'Life-cycle and environmental impact assessments on processing of plant fibres and its bio-composites: A critical review', *Journal of Industrial Textiles*, vol. 51, no. 4_suppl, pp. 5518S–5542S, Jun. 2022, doi: 10.1177/1528083720924730.
- [27] T. Béjat *et al.*, 'Design for the environment: SHJ module with ultra-low carbon footprint', *Progress in Photovoltaics: Research and Applications*, vol. 33, no. 1 Special Issue Article EUPVSEC 2023, pp. 184–199, Apr. 2024, doi: 10.1002/pip.3803.
- [28] 'Failure modes of silicon heterojunction photovoltaic modules in damp heat environment: Sodium and moisture effects', *Solar Energy Materials and Solar Cells*, vol. 278, p. 113190, Dec. 2024, doi: 10.1016/j.solmat.2024.113190.
- [29] T. Bejat *et al.*, 'Qualification of low environmental impact BOM for modules including a first feasibility study of wooden frames', Apr. 21, 2023. doi: 10.13140/RG.2.2.31197.32488.



Co-funded by
the European Union